AD NUMBER

ADB062483

LIMITATION CHANGES

TO:

Approved for public release; distribution is unlimited.

FROM:

Distribution authorized to U.S. Gov't. agencies only; Test and Evaluation; DEC 1980. Other requests shall be referred to Naval Postgraduate School, Code 012, Monterey, CA 93940.

AUTHORITY

NPS per DTIC form 55

NPS-67-80-020

NAVAL POSTGRADUATE SCHOOL

Monterey, California

THESIS

AERODYNAMICS AND CONTROL OF A 5"/54
GUN LAUNCHED MISSILE

by

John Stanton White

December 1980

Thesis Advisor: A.E. Fuhs

NAVAL POSTGRADUATE SCHOOL
Monterey, California

Rear Admiral J. J. Ekelund
Superintendent

David Schrady
Acting Provost

This thesis was prepared in conjunction with research supported in part by the Defense Advanced Research Projects Agency.

Released as a
Technical Report by:

William M. Tolles

W. M. Tolles
Dean of Research

UNCLASSIFIED

SECURITY CLASSIFICATION OF THIS PAGE (When Data Entered)

REPORT DOCUMENTATION PAGE

READ INSTRUCTIONS BEFORE COMPLETING FORM

1. REPORT NUMBER: NPS-67-80-020	2. GOVT ACCESSION NO.: AD B062483
3. RECIPIENT'S CATALOG NUMBER:	
4. TITLE (and Subtitle): Aerodynamics and Control of a 5"/54 Gun Launched Missile	5. TYPE OF REPORT & PERIOD COVERED: Master's Thesis; December 1980
	6. PERFORMING ORG. REPORT NUMBER: NPS-67-80-020
7. AUTHOR(s): John Stanton White	8. CONTRACT OR GRANT NUMBER(s): DARPA Order No. 4035
9. PERFORMING ORGANIZATION NAME AND ADDRESS: Naval Postgraduate School, Monterey, California 93940	10. PROGRAM ELEMENT, PROJECT, TASK AREA & WORK UNIT NUMBERS: Program Element No. 62702E; Work Unit No. 58056, Segment 1621/4.
11. CONTROLLING OFFICE NAME AND ADDRESS: Naval Postgraduate School, Monterey, California 93940	12. REPORT DATE: December 1980
	13. NUMBER OF PAGES: 103
14. MONITORING AGENCY NAME & ADDRESS(if different from Controlling Office): Naval Postgraduate School, Monterey, California 93940	15. SECURITY CLASS. (of this report): Unclassified
	15a. DECLASSIFICATION/DOWNGRADING SCHEDULE:

16. DISTRIBUTION STATEMENT (of this Report): Distribution limited to U.S. Government Agencies only; (Test and Evaluation); December 1980. Other requests for this document must be referred to the Superintendent, Naval Postgraduate School, Code 012, Monterey, CA 93940 ~~via the Defense Technical Information Center, Cameron Station, Alexandria, Virginia 22314.~~

17. DISTRIBUTION STATEMENT (of the abstract entered in Block 20, if different from Report): Approved for Public Release; Distribution Unlimited.

18. SUPPLEMENTARY NOTES:

19. KEY WORDS (Continue on reverse side if necessary and identify by block number):
Gun Launched Missile
Guided Projectile
Guided Projectile Aerodynamics
Reaction Jet Control

20. ABSTRACT (Continue on reverse side if necessary and identify by block number):

Analysis of the aerodynamics and jet reaction control of a 5"/54 gun-launched missile (GLM) was conducted. Aerodynamic analysis included estimation of lift and drag coefficients, lift-to-drag ratio, and center of pressure location by calculation for several versions of the missile at Mach numbers between Mach 2.0 and 3.0. Analysis included emphasis on compatibility with existing 5"/54 Mk 45 gun system. Jet reaction control

DD FORM 1 JAN 73 1473 EDITION OF 1 NOV 65 IS OBSOLETE S/N 0102-014-6601

UNCLASSIFIED

SECURITY CLASSIFICATION OF THIS PAGE (When Data Entered)

system investigation included calculation of the side force required to trim the missile for a 30-g maneuver at Mach 3.0.

Aerodynamics and Control of a 5"/54 Gun Launched Missile

by

John Stanton White
Lieutenant Commander, United States Navy
B.S., United States Naval Academy, 1969

Submitted in partial fulfillment of the requirements for the degree of

MASTER OF SCIENCE IN ENGINEERING SCIENCE

from the

NAVAL POSTGRADUATE SCHOOL
December 1980

Author _____

Approved by: _____
Thesis Advisor

_____
Second Reader

_____
Chairman, Department of Aeronautics

_____
Dean of Science and Engineering

ABSTRACT

Analysis of the aerodynamics and jet reaction control of a 5"/54 gun-launched missile (GLM) was conducted. Aerodynamic analysis included estimation of list and drag coefficients, lift-to-drag ratio, and center of pressure location by calculation for several versions of the missile at Mach numbers between Mach 2.0 and 3.0. Analysis included emphasis on compatibility with existing 5"/54 Mk 45 gun system. Jet reaction control system investigation included calculation of the side force required to trim the missile for a 30-g maneuver at Mach 3.0.

TABLE OF CONTENTS

LIST OF TABLES

LIST OF FIGURES

ACKNOWLEDGEMENT

The author would like to acknowledge the support of the Defense Advanced Research Projects Agency for providing the necessary funding to conduct this research project.

The author would also like to express his sincere appreciation to Dr. Allen E. Fuhs, Distinguished Professor of Aeronautics and Physics and Chemistry. Through his guidance and patience, Dr. Fuhs was the consistent, steady driving force to enable this student to complete this project.

The student would also like to thank Mrs. Emily Fuhs for her ability to critique effectively the grammatical content of the thesis and ensure that all difficult concepts were expressed in the clearest manner.

Finally, the author would like to thank his wife for her extreme patience during this undertaking. Without her continued support during the project, difficult obstacles might not have been overcome.

I. INTRODUCTION

Since the attack and destruction of the Israeli destroyer "Elath" in 1968 by four Soviet built SSN-2 Styx missiles fired from Egyptian missile boats, the U.S. Navy has been searching for combat capabilities to counter the anti-ship cruise missile threat. In this effort, the capabilities of the combat systems developed have ranged from the close-in self defense systems with kill range capabilities of only several miles to the recently developed, multi-faceted multi-threat Aegis system with its SM-2 missiles capable of intercepting potential missile threats 60 miles [1] from the firing ship.

In this twelve year effort, one area the Navy has failed to exploit fully is the development, production, and deployment of a combat system that (1) has the capability to intercept and destroy the cruise missile threat with a reasonable P_k (probability of kill) in the current and near term environment, (2) has a wide and immediate applicability to the currently existing fleet assets, (3) has a medium self-defense range capability, and (4) still has affordability vis a vis the existing alternatives.

A combat capability that may meet the four criteria mentioned previously is the 5"/54 gun-launched missile (GLM) currently being investigated by offices in the Naval Sea Systems Command, this student, and private contractors.

The 5"/54 GLM is a relatively low cost combat system with immediate applicability to every 5"/54 Mk 45 capable ship in the fleet with or without a surface to air capability. The GLM will increase significantly the anti-ship missile defense (ASMD) capability over the conventional anti-air gunnery abilities currently existing.

The purpose of this thesis is to investigate two major aspects of the GLM. The first major section addresses the aerodynamics of several configurations proposed as gun-launched missiles. Refer to the theses of Parks [2], Frazier [3], and Brown [4] for additional information concerning the GLM. The second major section addresses the field of jet reaction control as a potential control system in a GLM.

II. BASIC ASSUMPTIONS AND DESIGN CONSTRAINTS

Basic aerodynamic and reaction jet control assumptions and decisions for the 5"/54 caliber gun-launched missile (GLM) were made at the beginning of this thesis investigation. These assumptions and decisions were made on the basis of mission applicability and subsystem requirements and are described below.

Ground Rules: Ground rules were defined for both the 5"/54 (GLM) and the gun; the ground rules are now discussed.

Missile: The missile flight profile was considered to be as follows:

- Launch, with immediate de-spin at muzzle exit
- Powered ballistic flight throughout trajectory to intercept, utilizing the concept of thrust equal to drag
- Launch velocity at the speed corresponding to no change in the powder case propellant characteristics, i.e. approximately 2100 fps
- Missile maneuver capability of 30 g's at Mach 3 and sea level
- Flight time of approximately 20 seconds and range limits of 10 nm on the trajectory
- Reaction jet control or combination tail/reaction jet control
- Maximum angle of attack limited only by the axially symmetric inlet

Gun: In accordance with the physical characteristics of the 5"/54 caliber, Mk 45 lightweight gun, the missile was to be no greater than 61 inches in length and be able to interface

with existing loading system constraints. The gun constraints force a bottleneck configuration in the forebody of the missile.

Subsystem Assumptions: For realistic aerodynamic and jet control configurations, basic assumptions were made about the types and characteristics of the non-aerodynamic subsystems. Some of the subsystems are dealt with extensively in the companion reports [2, 3, 4] to this thesis. The subsystems, however, are addressed to some extent below, as they pertain to the aerodynamic and control packages in this thesis.

Propulsion: Integral rocket ramjet propulsion system was assumed with ignition immediately after launch.

Warhead: A fragmenting warhead capable of defeating an air target with the capabilities predicted for the 1980-1990 time-frame was assumed.

Structure: An overall structural ability to withstand launch from the 5"/54 gun was assumed.

Sensor: An active sensor system located in the forebody of the missile capable of opposing an air target with the capabilities predicted for the 1980-1990 time frame was assumed.

III. AERODYNAMIC THEORY

A. INTRODUCTION TO AERODYNAMIC DESIGN

In determining the optimum aerodynamic properties of a particular flight vehicle, the aerodynamicist has several options. One method is construction of scale models of the various proposed designs for testing, with the result being a determination of the optimum configuration, aerodynamically, to meet the mission requirements and still interface with all other system requirements and assumptions. Unfortunately, even scale models have become increasingly cost prohibitive in these days of high inflation; and at the very least, the model construction consumes considerable time. More frequently, the aerodynamicist undertakes a feasibility study analytically, using existing aerodynamic and gas dynamic theory, calculating the required parameters of lift, drag, center of pressure, etc., based on the particular shapes imagined for the prescribed mission. Then, after iteration with the other requirements of the flight vehicle, a configuration design is built and tested.

In this thesis, the aerodynamic configurations of several options for the 5"/54 gun-launched missile (GLM) were undertaken through aerodynamic theory.

Calculations for each particular area of concern for the missile were conducted. Finally, the calculated values for

each proposed GLM configuration were presented.

For each GLM configuration, the particular vehicle was divided into four of the five major areas which affected the drag and lift of the vehicle. The five major areas which affect the drag and lift of a given flight vehicle are 1) the nose, 2) the body, 3) the wings or fins, 4) the base, and 5) aerodynamic interference. Each component contributes to the overall drag and lift characteristics which ultimately determine the aerodynamic capability of the missile. Aerodynamic interference, which is discussed by Nielsen [5], has not been considered.

In this initial design effort, three iterative aerodynamic configurations were chosen for study and evaluation; each configuration met the general assumptions and ground rules discussed earlier for GLM application. The configurations were propelled by ramjet engines using axially symmetric nose inlets. The aerodynamic forces were divided into two areas of concern, external aerodynamics and internal aerodynamics. This thesis considers external aerodynamics.

B. NOSE LIFT

Recall from the introduction to aerodynamic theory that the nose of the flight vehicle is a contributor to the aerodynamic lift of a body.

Since the nose inlet configurations were dictated by the ramjet engine propulsion system, the lift due to this particular geometry had to be considered. Hoerner [6] states that

lift is that force which is due to the pressure distribution over the body in a direction normal to the freestream velocity.

For both GLM Configurations I and II, Figure 1 depicts the chosen inlet geometry. Although the overall dimensions were slightly different in each configuration, the relative configurations are the same for aerodynamic purposes.

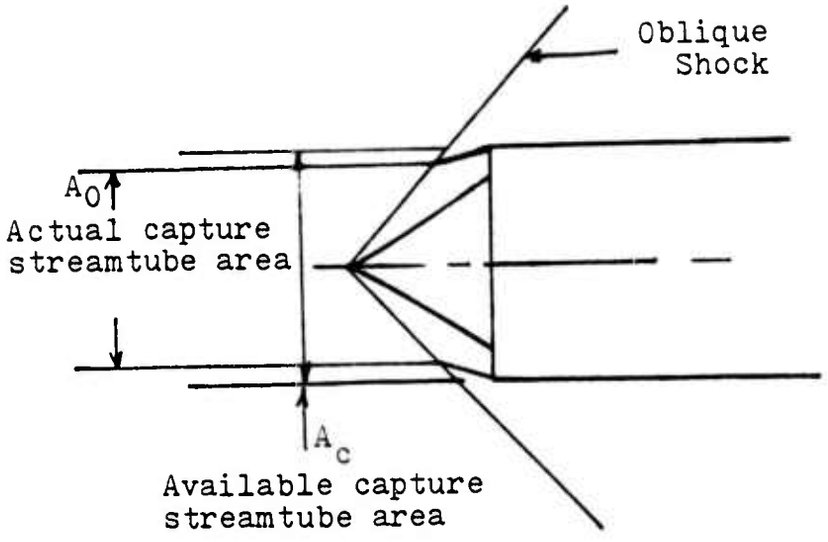

Figure 1. Forebody and inlet of Configurations I and II.

To analyze and determine the lift generated by the inlet nose of the GLM, Newton's second law of motion is needed. Considering motion of an isolated body, the law states that the summation of the forces exerted on a body at a certain instant is equal to the rate of change in momentum of the body at that instant. Hoerner [6], however, modifies the situation in that for a stream of air, there is not an isolated finite mass; rather, there is a mass flow. Momentum

is transferred, as one would expect, onto the passing stream of air by adding a vertical component of velocity.

In order to determine the force created by the nose inlet, the inlet was modeled analytically as a control volume with a constant mass flux and a change in direction of flow equal to the angle of attack α. Figure 2 depicts the dynamics.

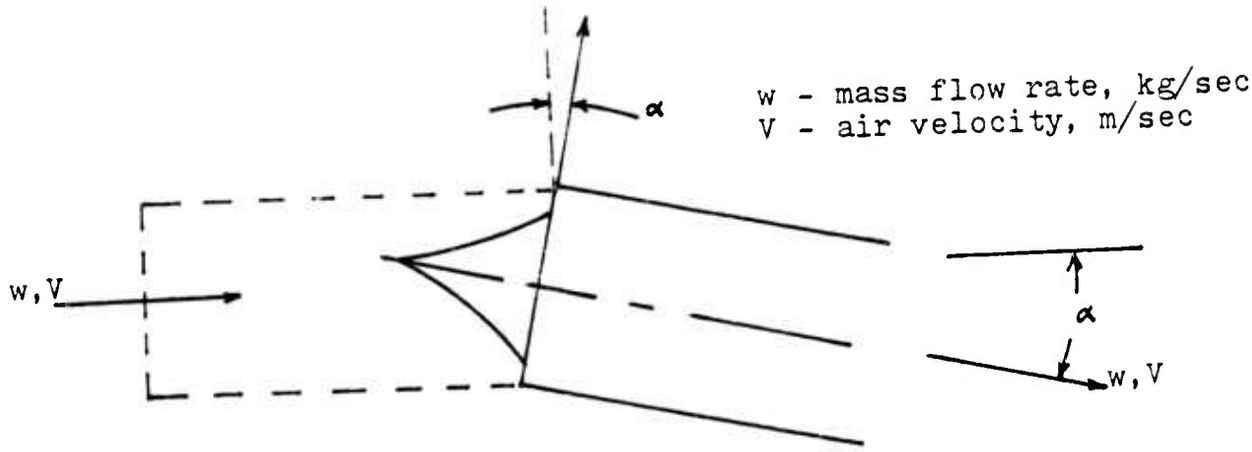

Figure 2. Analytical model for nose lift.

From the geometry of Figure 2 and the momentum equation, the lift L is

$$L \doteq wV\sin\alpha \qquad (1)$$

where w is the mass flow rate, kg/sec; and V is the velocity of the air, m/sec. For very small angles, the sine of the angle may be approximated by the angle. For small angles of attack α, $\sin\alpha$ is approximately α. Therefore

$$L \doteq wV\alpha$$

By the continuity equation[1], the mass flow rate w is equal to the product of the density ρ of fluid, kg/m^3, the area S through which the fluid passes, m^2, and the velocity V of the fluid. By inserting the values of the product equal to w into equation (1),

$$L = \rho V^2 S\alpha \tag{2}$$

Hoerner [6] states that lift can be represented as the product of the dynamic freestream pressure, q, N/m^2, the area S previously defined and a non-dimensional term called the coefficient of lift, C_L. The dynamic freestream pressure is shown in equation (4).

$$L = C_L\, qS \tag{3}$$

$$q = \tfrac{1}{2}\rho V^2 \tag{4}$$

By substituting equation (4) into equation (3), the general term for the coefficient of lift can be determined. This is shown in equation (5). By substituting equation (2) into equation (5), the coefficient of lift can be determined for the nose section of the GLM.

$$C_L = \frac{L}{\rho V^2 S/2} \tag{5}$$

$$C_L = \frac{\rho V^2 S\alpha}{\rho V^2 S/2} = 2\alpha \tag{6}$$

---

[1]For more information on the continuity equation, Liepmann and Roshko [7] is an excellent reference.

For the configurations studied in this thesis, C_L for a given angle of attack α are tabulated in Section V.

For Configuration III, Figure 3 depicts the chosen inlet geometry. The aerodynamic cowling was a result of the design process. Not all of the incoming volume of air could be utilized by the ramjet engine; consequently, the capture streamtube area, A_0, was reduced. For the iteration from Configuration I to III, the dimensions were sufficiently different to warrant investigation of alternative methods for calculating the lift coefficient resulting from the nose configuration. The major geometrical difference between Configuration I and Configuration III is the cowling shown in Figure 3. The lift contribution due to the air which enters the ramjet was calculated using equation (6). For the calculation of the cowling lift, the computer program of Tillotson and Schonberger [8] was used. For an angle of attack of 5 degrees, the program gave C_L due to the cowling significantly less than the other contributions to C_L.

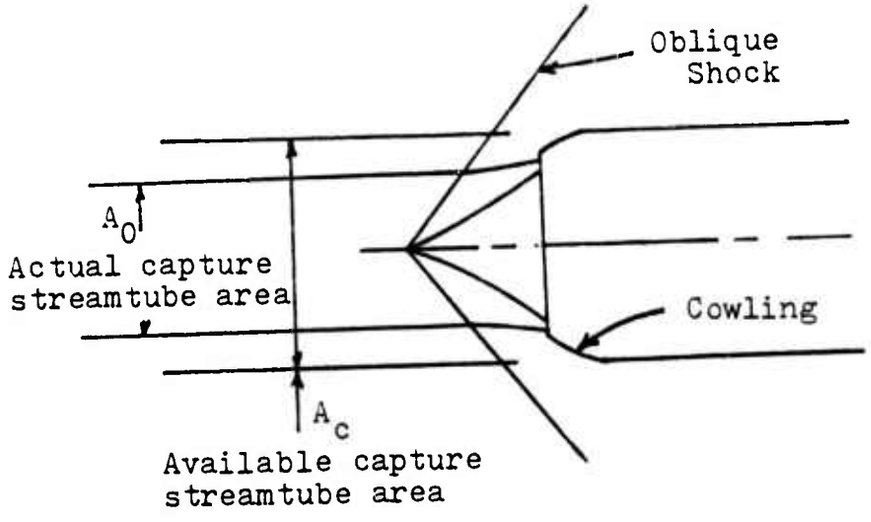

Figure 3. Nose and forebody of Configuration III with redesigned cowling.

Consequently, the cowling lift was ignored in subsequent calculations. As a word of caution, the importance of cowling lift should be investigated in more detail. The lift coefficient for given angles of attack also is tabulated in the design section.

C. NOSE DRAG

For any aerodynamic configuration, the nose or forebody can cause significant drag. Since, in this design study, the GLM configurations were powered by ramjet engines with an axially symmetric inlet, the inlet geometry was chosen such that the nose drag was minimal, i.e., the mass flow ratio A_0/A_c as depicted in Figures 1 and 3 was as close to unity as possible. Thus, for both Configuration I and II, the drag coefficient for the nose was assumed to be equal to zero at an angle of attack α equal to zero.

After the initial design efforts, however, modification of the nose design was necessary as the mass flow ratio A_0/A_c depicted in Figure 1 was not suitable for the ramjet engine. Figure 3 depicted the revised design. Calculation of the nose drag due to the cowling was made based on a computer program developed by Tillotson and Schonberger [8].

D. BODY DRAG

The body drag of a flight vehicle is composed of two major factors: drag due to the friction of the body and drag as a result of the configuration or shape of the body.

In this thesis, Configuration I total drag was affected only by the friction drag. Configurations II and III were affected by both factors of body drag. Both form drag (pressure) and skin friction drag were considered in the aerodynamic analysis.

Hoerner [9] states that the pressure drag is that force which represents the streamwise component of the pressure integrated over the entire configuration. In contrast, the skin friction drag is that force obtained by integrating the streamwise component of the shear stress over the flight vehicle. In order to calculate the skin friction drag of a particular body, the following equation is defined:

$$\text{Drag} = \int \tau n_y dS$$

where τ is the local skin friction, N/m^2, n_y is the local y-component of the normal vector to the surface and dS is an element of area, m^2. Fluid flow is in the x-direction. In this thesis, an approximation of the equation for skin friction was made.

$$\text{Drag} = \tau S_r \tag{7}$$

In equation (7), S_r represents the reference area. The approximation was a result of averaging the shear stress over the entire surface of the body. The average shear stress τ is defined

$$\tau = q\, C_{fc} \tag{8}$$

where q is the dynamic freestream pressure previously defined on page 19 and C_{fc}, the coefficient of friction for compressible fluid flow. For more information on the momentum and

energy equations that define the dynamic pressure, the reader is referred to references [7, 10,11].

Recall that for a perfect gas

$$p = \rho RT \tag{9}$$

and the speed of sound is defined as

$$a = \gamma RT \tag{10}$$

where γ = ratio of specific heats

R = specific gas constant, $\frac{m^2}{s^{2}{}^{o}K}$

Since the definition of Mach number is

$$M = V/a \tag{11}$$

by substituting equations (9), (10) and (11) into equation (4), the dynamic pressure becomes

$$q = \gamma p M^2/2 \tag{12}$$

In order to calculate the average shear stress over the body and ultimately the skin friction drag, the aerodynamicist must determine C_{fc}. Usually this coefficient is determined by finding the coefficient of friction in an incompressible flow and then adjusting for compressible flow. In discussing fluids of both an incompressible and compressible nature, viscosity should be addressed. Shear stress can be defined as proportional to the rate of angular deformation of a given fluid. The proportionality constant in the equation is defined as the viscosity of the fluid. Dimensions for viscosity are Newton-seconds per square meter.

The ratio of inertia forces to viscous forces on a body in a fluid flow is defined as the Reynolds number

$$Re = \frac{\rho V L}{\mu} \qquad (13)$$

L = the appropriate characteristic length of the vehicle under analysis, m

μ = viscosity of the fluid through which the vehicle is passing, N - S/m^2

Since the fluid through which the GLM passes is air, the viscosity of air for the particular altitude or altitudes at which the GLM operates is needed. Figure 4 depicts the Reynolds number per characteristic length L as a function of velocity and altitude for U.S. Standard Atmosphere. The characteristic length L was equal to one meter.

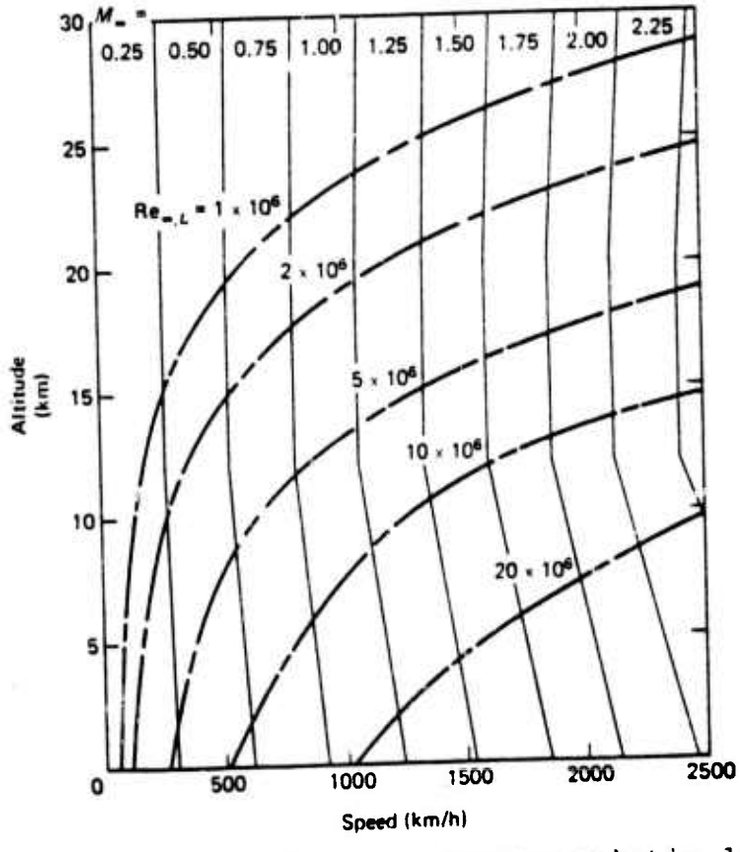

Figure 4. Reynolds number per characteristic length as a function of velocity and altitude for U.S. Standard Atmosphere. From Bertin and Smith [10]

Hoerner [9] states that outside of the boundary layer, the effects of the shear forces are negligible. Because of this, the region outside of the boundary layer is treated as inviscid flow. For airfoils passing through air, a complex flow pattern develops as the velocity of the flight vehicle increases. The boundary layer is divided into two portions: (1) a laminar portion and (2) turbulent portion. In general, the laminar portion of the boundary layer is that region where the "layers" of gas do not mix with each other and are parallel to each other with steady velocities.

The turbulent portion, in contrast, as Hoerner [9] states, is that portion in "a constant 'state of commotion and agitation', consisting of velocity fluctuations superimposed to the main flow. Turbulent flow occurs within boundary layers (at higher Reynolds numbers) and within the wake behind solid bodies." For vehicles at high Reynolds numbers and high velocities, the flow is characterized by a laminar portion of the boundary layer that then transitions through a finite region to a turbulent portion of boundary layer. Figure 5 illustrates this complex transition.

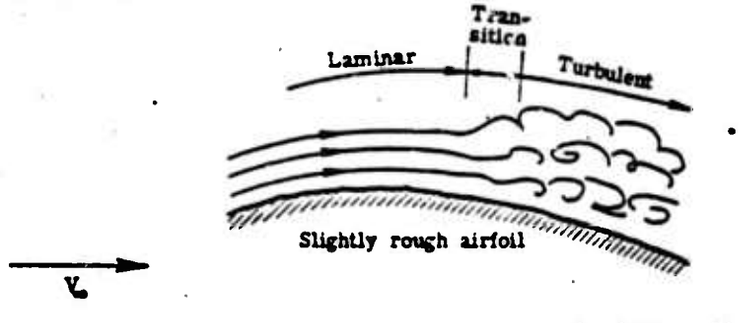

Figure 5. Transition from laminar to turbulent fluid flow over airfoil. From Talay [12]

Thus, in the laminar region

$$D_\ell = C_{f_\ell} qS_\ell \tag{14}$$

and in the turbulent region

$$D_t = C_{f_t} qS_t \tag{15}$$

The coefficient of friction for laminar incompressible flow has been determined empirically [6, 9] to be

$$C_{f_\ell} = 1.328/\sqrt{Re} \tag{16}$$

In a similar manner, Schoenherr, in Hoerner [9], established an equation which is used for calculating the turbulent coefficient of friction for incompressible flow and is valid up to the highest Reynolds numbers normally encountered in engineering, i.e., around 10^9. The Schoenherr equation is

$$\log_{10}(ReC_f) = 0.242/C_f^{\frac{1}{2}} \tag{17}$$

For a given Re, an iterative process is conducted until both sides of the equation are balanced, which determines the C_f.

Thus, the drag due to skin friction on the body of the flight vehicle in incompressible flow is

$$D = qC_{f_\ell} S_\ell + qC_{f_t} S_t \tag{18}$$

If x* is defined as the distance from the leading edge or nose of the body to the point at which laminar flow changes to turbulent flow, and if the surface area of the entire body is S(L), then

$$\text{Drag} = q\, C_{fi} S(x^*) + qC_{ft}\, [A(L) - A(x^*)] \tag{19}$$

since A(L) - A(x*) would be the surface area of the turbulent region.

The distance x* along the body at which the transition occurs is given by

$$x^* = \frac{\mu \, Re^*}{\rho \, V} \tag{20}$$

where Re^* is the Reynolds number at transition.

For Reynolds numbers greater than 1 or 2 million, based on the total length of a given body, Hoerner [9] plots a Re^* of 2×10^6.

Once the coefficient of friction for an incompressible flow is found, it is adjusted for compressibility of air, since the GLM is traveling [illegible]ically through the air. An equation from Hoerner [9] was used for adjusting from incompressible to compressible flow.

$$C_{fc}/C_{fi} = (1 + 0.15M^2)^{-0.58} \tag{21}$$

Calculation of a coefficient of friction for compressible flow at a given Mach number is accomplished by using the C_{fi} discussed earlier.

Finally, returning to equation (8),

$$\tau = q \, C_{fc}$$

the average shear stress over the surface of the body is calculated; and using equation (7), the drag of the body due to friction is determined.

For Configuration I, in which the body drag was due solely to skin friction, the calculations are discussed in detail. SI units were used; and the density, pressure, and temperature values for the GLM at sea level [6] were used in the calculations.

Since several configurations were investigated in this thesis, and each was evaluated at various velocities and altitudes, a computer program using the HP 9830 was developed. This program is discussed in greater detail in Section IV.

E. BODY LIFT

The missile designer chooses a slender, streamline shape to minimize the drag on the body, as has been shown already in the section on body drag. One additional, positive side effect is that the streamline shape also produces a lift on the body. Body lift was calculated for the GLM configurations investigated. According to Hoerner [6], for streamline bodies such as GLM configurations analyzed in this thesis, the lift consists of two separate components, one due to circulation and the other due to cross flow.

In a slender body of revolution, such as the cylindrical mid section of the GLM body, the lift coefficient for low angles of attack α is

$$C_L = \sin(2\alpha) = 2\sin\alpha\cos\alpha$$

For small angles, C_L reduces to

$$C_I \doteq 2\alpha$$

As the angle of attack increases above a few degrees, the component of flow normal to the body becomes more significant. The second component of body lift is proportional to the cross-flow coefficient known as

$$C_c = C_n = C_{90}$$

for several of its names. The proportionality will be shown explicitly in equation (22). Hoerner [6] states that at very high Reynolds numbers, such as Re = 10^6, experimental results indicate C_{90} between 1.1 and 1.2 for the type cylinder depicted in Figure 6. The data for the results are presumed to be for subsonic flow.

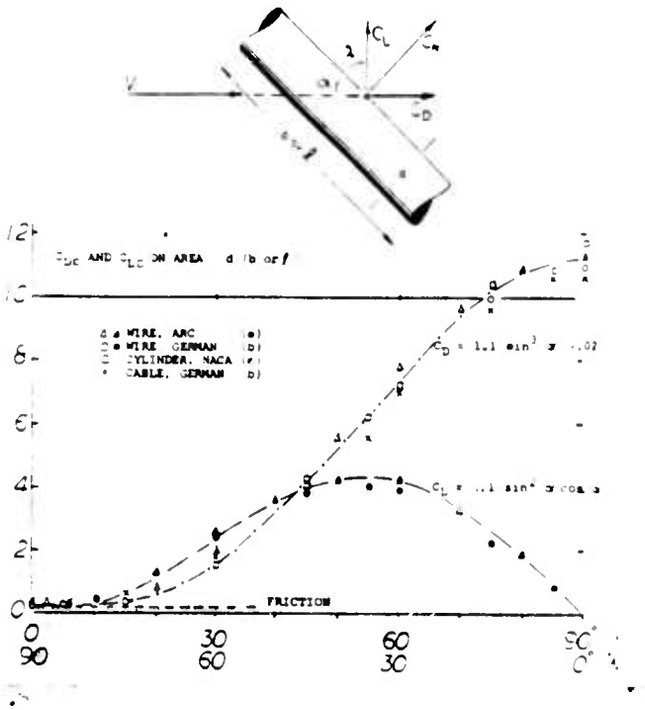

Figure 6. Cross-flow coefficient versus angle of attack for cylinders in subsonic flow. From Hoerner [6].

The equation used to calculate the normal force coefficient is

$$C_N = 2\alpha + C_{90} \frac{S_p}{S_r} \alpha^2 \qquad (22)$$

The ratio S_p/S_r is the ratio of the presented area to the reference area. For more information on the theory and the

experimental results, the reader is referred to Hoerner [6].

As shown in Appendix C, lift L is nearly equal to the normal force N when the angle of attack is small and the lift-to-drag ratio is large. Since all the configurations were considered to be operating in the low angle of attack regime with large L/D, the body normal force was considered approximately equal to the body lift coefficient.

Lift coefficients as a result of the body normal forces for all configurations are tabulated in the design section.

F. TAILFIN DRAG

The drag of the airfoil is a result of two force components. These two forces are called wave (or form) drag and friction drag.

The theory defining friction drag has been discussed already. Detailed calculations relevant to the particular configurations are tabulated in Section V. Wave drag is due to a pressure exerting a drag on the GLM fins and therefore is discussed in its entirety.

For the GLM, a slender double-wedge airfoil in supersonic flow, as shown in Figure 7, was considered since the flight range was Mach 2.0 to Mach 3.0.

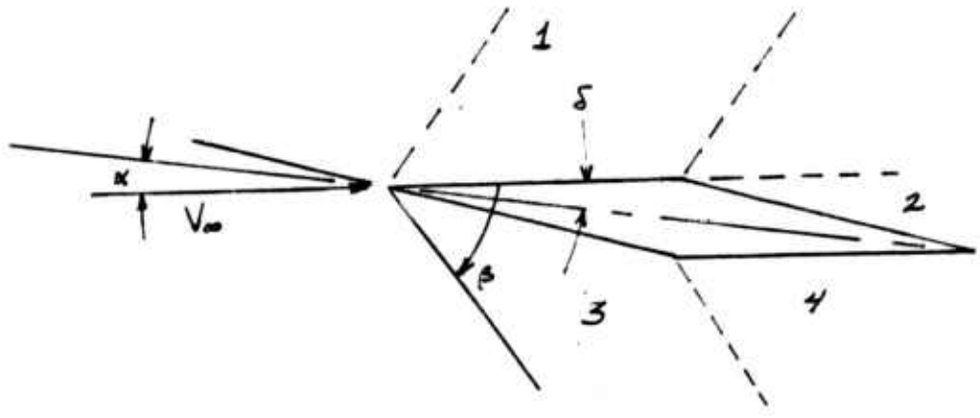

Figure 7. Double-wedge airfoil at angle of attack.

For the double-wedge airfoil which is depicted in Figure 7 the supersonic flow causes the formation of a shock wave that is attached to the leading edge of the airfoil. In addition, the wave is planar, and the downstream flow is isentropic. A technique called the shock expansion theory was used [10] to calculate the section drag coefficient and similarly the section lift coefficient for the double-wedge airfoil. Liepmann and Roshko [7] state shock-expansion theory uses the principle that the oblique shock wave and simple isentropic wave furnish the building blocks for analyzing problems in two-dimensional supersonic flow. Key to the theory is attachment of the shocks. The two-dimensional theory ignores wing tip unloading, and this thesis will not address wing tip unloading for the GLM. More information on shock-expansion theory is provided in Refs. [7, 10, 11] .

The geometry of the chosen fin for the GLM was represented in Figure 7. The calculations, shown for example purposes to illustrate the theory, used the geometry of this fin. Sample calculations are for an angle of attack α equal to 5 degrees.

From Figure 7, the surface in region 1 is parallel to the freestream condition. The flow does not turn; and consequently, the flow properties in region 1 are the same as freestream. The pressure coefficient on the airfoil surface bounding region 1 is zero. Thus, $M_\infty = M_1 = 3.0$, the Prandtl-Meyer angle $\nu_1 = 49.75^\circ$, $\theta_1 = 0^\circ$ and $C_{p1} = 0$.

Since the surface of the airfoil in region 2 turns away from the flow in region 1, the flow accelerates isentropically in going from region 1 to region 2. From Figure 7 $d\nu = -d\theta$; and since $\theta_2 = -10^\circ$, $\nu_2 = \nu_1 - \Delta\theta$, and $\nu_2 = 59.75^\circ$. Using compressible air flow tables [14], $M_2 = 3.58$.

To calculate the coefficient of pressure in region 2, the Prandtl-Meyer relation discussed in Liepmann and Roshko [7] is used. Equation (23) gives the coefficient of pressure desired.

$$C_{p2} = \frac{p_2 - p_\infty}{(\gamma/2)\, p_\infty M_\infty^2} = \frac{2}{\gamma M_\infty^2}\left(\frac{p_2}{p_\infty} - 1\right) \qquad (23)$$

Since the flow over the upper surface of the airfoil is isentropic, the stagnation pressure is constant, and $p_{t\infty} = p_{t1} = p_{t2}$. Therefore equation (23) becomes

(24)

$$C_{p2} = \frac{2}{\gamma M_\infty^2} \left(\frac{P_2}{P_{t2}} \frac{P_{t\infty}}{P_\infty} - 1 \right) \qquad (24)$$

Using the values for the airfoil considered, $C_{p2} = -0.0904$.

Turning to the lower surface of the airfoil, the pressure coefficients for regions 3 and 4 may be calculated.

When supersonic flow encounters a change in direction resulting in compression, the flow decelerates, and a shock wave occurs [7, 10, 11]. The shock wave is a discontinuity in the continuation of the flow. These discontinuities may be large or small, hence the notion of "strong" or "weak" shock waves. Since the shock wave is usually thought of as a large pressure wave, [11] the term "pressure jump" is used as a measure of shock strength.

Various parameters may be used to measure the shock strength. Since the flow through the shock wave is adiabatic, [7, 10, 11], the entropy must increase as the flow passes through the shock wave. Two of the parameters by which the shock wave may be measured are the shock wave angle β and the deflection angle δ. The following relation exists between these two angles:

$$\cot \delta = \tan \beta \left[\frac{(\gamma + 1) M_1^2}{2(M_1^2 \sin^2 \beta - 1)} - 1 \right] \qquad (25)$$

Figure 8 depicts the appropriate angles and symbols.

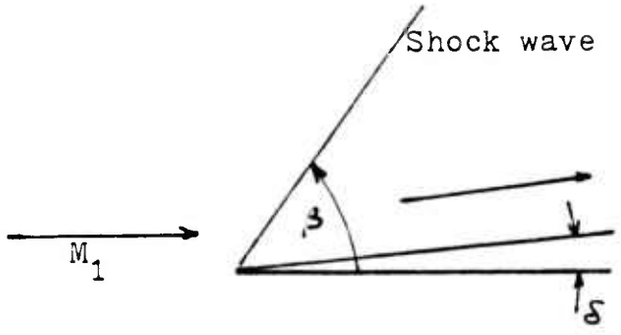

Figure 8. Shock wave angle and deflection angle in supersonic flow.

Since the deflection angle δ is known for the airfoil under consideration, the shock wave angle β can be calculated. Using equation (25), $\beta = 27.5^{\circ}$. The pressure jump can be found in region 3 by $M_{\infty}\sin\beta = M_n$ and the tables. For the example airfoil, $M_n = 1.385$, and $p_3/p_{\infty} = 2.071$. Using equation (24), $C_{p3} = 0.1700$.

The calculation of M_3 can be accomplished by using equation (26) with $\delta = 10^{\circ}$.

$$M_3 = \frac{(\gamma - 1)\, M_{\infty}^2 \sin^2\beta + 2}{[2\gamma M_{\infty}^2 \sin^2\beta - (\gamma - 1)]\, \sin^2(\beta - \delta)} \qquad (26)$$

Inserting the necessary values yields $M_3 = 2.48$; and from the tables $\nu_3 = 38.75^{\circ}$.

Since from Figure 7, $\Delta\theta = 10^{\circ}$ between region 3 and region 4, $\nu_4 = 48.75^{\circ}$.

Returning to the tables with the Prandtl-Meyer angle, $M_4 = 2.95$; and by using equation (24) once more, $C_{p4} = 0.0011$.

Having determined the pressures on the individual regions of the thin double-wedge airfoil, the section drag coefficient can be determined. This is the drag coefficient for an airfoil with unit span. Using the fact that the net force in any direction due to constant pressure acting on a closed surface is zero, [10] the pressure coefficients may be summed around the surface of the airfoil as in equation (27) to find the section drag coefficient

$$C_{d'} = \frac{1}{2\cos\delta} \sum C_p \sin\theta \qquad (27)$$

In this case $C_{d'} = 0.0075$. Once the section drag coefficient is determined, the drag coefficient can be calculated by multiplying the value by the span b, measured in meters, of the airfoil.

$$C_d = C_{d'} b \qquad (28)$$

For the GLM fin under consideration, $C_d = 0.0013$.

The coefficient of drag for each tailfin is based on the fin area as the reference area. For this value to be applicable to the GLM under consideration, it must be converted to a drag coefficient based upon the reference area for the GLM. As discussed earlier, the reference area for the GLM is the base area. Thus, the drag coefficient as a result of the sum of all four tailfins was multiplied by the tailfin reference area divided by the base area. Results for the tailfin configurations selected are tabulated in Section V.

G. TAILFIN LIFT

For thin airfoils, such as the double-wedge airfoil to be used in the GLM configuration, the section lift coefficient is found as a result of the same technique as used in calculating the section drag coefficient. Once the missile designer determines the pressures of the individual regions of the airfoil, the lift coefficient for the section of the airfoil shown in Figure 7 can be determined. Equation (29) shows how the section lift coefficient is calculated.

$$C_{L'} = \frac{1}{2 \cos \delta} \sum C_p \cos\theta \qquad (29)$$

Once the section lift coefficient is determined, the lift coefficient can be calculated by multiplying the section lift coefficient by the span of the airfoil under consideration.

As was discussed in the section on tailfin drag, the coefficient of lift for each tailfin is based on the reference area for the fin. This coefficient also had to be converted to a lift coefficient based on the reference area of the GLM. Thus, the lift coefficient based upon the lifting surfaces of two tailfins was multiplied by the factor of the tailfin reference area divided by the base area. Results for the tailfin configurations are tabulated in Section V.

IV. AERODYNAMIC DESIGN CALCULATIONS

A. INTRODUCTION

This section of the thesis considers the detailed calculations for the aerodynamic values for one of the several configurations. Sample calculations are illustrated for the representative sections contributing to lift or drag on Configuration I. Additionally, the several computer programs utilized in this thesis to aid in more rapid calculations of subsections of each configuration are discussed and presented.

In the course of the aerodynamic analysis, calculations for several sections of each configuration were identical except for the basic parameter involved. The calculations presented in this section are designed to illustrate and amplify the aerodynamic theory formally presented in Section III. Sample calculations presented in this section are representative in nature, and not every value tabulated in Section V is treated. Rather the purpose of this section is to illustrate explicitly how the design of the several configurations for this thesis was approached. Methodology is emphasized, and the fact that in all analytical endeavors some plain "number crunching" must be done is illustrated.

B. SECTION CALCULATIONS

Calculations for each component of Configuration I are presented in this section. Table I provides the geometric data for Configuration I. TableII provides the standard atmospheric values used in many of the calculations.

TABLE I

CONFIGURATION I GEOMETRIC DATA FOR CALCULATIONS

BODY:		TAILFIN:	
Length, overall, m	1.3716	Area (2 panels), m^2	0.0121
Diameter, m	0.1270	Chord, m	0.0635
Volume, m^3	0.0164	Span, m	0.09525
Wetted Area, m^2	0.5168	Thickness ratio	0.0875
Base area, m^2	0.0127	Aspect ratio	1.499

TABLE II

STANDARD ATMOSPHERIC VALUES FOR AIR AT SEA LEVEL

$\delta = 1.225\ kg/m^3$

$T = 288.2^{o}K$

$P = 101,300\ N/m^2$

$\lambda = 1.4$

1. Calculation of Body Drag

From the data in Table I, the surface area of the body was calculated,

$$A_s = dL = 0.5168 \text{ m}^2 \tag{30}$$

and the dynamic freestream pressure was determined

$$q = \tfrac{1}{2} \rho V^2 = 637,245 \text{ N/m}^2 \tag{31}$$

The Reynolds number which was defined in equation (13), was found to be

$$Re = \frac{(1.225)(1020)(1.2954)}{1.8 \times 10^{-5}} = 89.9 \times 10^6 \tag{32}$$

Since the Reynolds number is greater than the transition Reynolds number, the body has turbulent flow; refer to Section III for a discussion of boundary layer transition. Recall from the theory that for incompressible flow in a turbulent boundary layer

$$\log_{10}(Re\ C_f) = 0.242/C_f^{\frac{1}{2}} \tag{33}$$

where C_f is the coefficient of friction. Equation (33) is solved iteratively using the Reynolds number from equation (32).

$$C_f = 0.00211$$

For the adjustment from incompressible to compressible flow, equation (34) is used where M = 3.0.

$$C_{fc} = C_{fi} (1 + 0.15\ M^2)^{-0.58} \tag{34}$$

After inserting the incompressible value in equation (34), C_{fc} was determined to have a value of 0.001285. Recall from the discussion of body drag that the shear stress τ was defined as $\tau = q\ C_{fc}$. Inserting numerical values gives

$\tau = 818.26$.

Finally, using equation (7), drag = τA_s = 423.2 N and $C_D = D/qS_{ref}$ = 0.0524.

Modifying a program developed for the NPS course AE 4705, [13] the above steps were programmed for the HP 9830 computer. The program is listed in Table III with a sample output in Table IV. With inputs of velocity, diameter, length and altitude, the program calculates the body skin friction drag of a cylindrical body.

TABLE III

HP 9830 PROGRAM TO CALCULATE BODY DRAG; PROGRAM STEPS

```
10 PRINT "THIS PROGRAM CALCULATES PROJECTILE BODY DRAG."
20 PRINT "THIS PROGRAM IA STORED IN FILE 0."
30 PRINT ""
40 DEG
50 D1=100
60 DISP "PRINT INPUT?YES=1 NO=0";
70 INPUT K
80 PRINT
90 PRINT "FOR SUPERSONIC VELOCITY INSERT 0."
100 PRINT
110 DISP "SEE PRINTED STATEMENT CONCERNING VELOCITY";
120 INPUT K9
130 D1=100
140 D=0.12598
150 R=D/2
160 A=PI*R↑2
170 A1=340
180 V=1020
190 M=V/A1
200 H=7620
210 Y=0
220 PRINT "**************************"
230 PRINT "ALTITUDE IS";Y"METER"
240 R0=1.225
250 Z=R0*EXP(-Y/H)
260 M7=1.8E-05
270 R1=2E+06
280 X=(R1*M7*EXP(Y/H))/(R0*V)
290 L=1.5494
292 IF K9=0 THEN 310
310 S3=2*PI*L*R
320 IF L>X THEN 350
330 S=S3
340 GOTO 420
350 S=2*PI*R*X
420 C1=1.328/(SQR(R1))
425 C1=C1/((1+0.45*M↑2)↑0.25)
430 R2=R1*(L/X)
440 PRINT "    "
450 Q1=C1
460 Q2=LGT(Q1*R2)
470 Q3=Q2↑2
480 Q4=0.058564/Q3
490 Q5=ABS(Q4-Q1)
500 IF Q5<1E-06 THEN 585
510 IF Q5<1E-05 THEN 570
520 IF Q5<1E-04 THEN 550
530 Q1=Q1+C1/D1
540 GOTO 460
```

TABLE III (CONTINUED)

```
550 Q1=Q1+C1/(5+D1)
560 GOTO 460
570 Q1=Q1+C1/(40+D1)
580 GOTO 460
585 Q1=Q1/((1+0.15*M↑2)↑0.58)
590 Q9=R0*(V↑2)*(0.5)*EXP(-Y/H)
600 D7=Q9*(C1*S+Q1*(S3-S))
610 C7=D7/(Q9*A)
670 IF K9=1 THEN 700
750 IF K=0 THEN 940
760 IF K9=1 THEN 790
780 GOTO 800
800 PRINT "PROJECTILE LENGTH";L"METER"
810 PRINT "PROJECTILE DIAMETER";D"METER"
830 PRINT "BASE AREA";A"METER SQUARED"
840 PRINT "SPEED OF SOUND";A1"VELOCITY OF PROJECTILE";V"METER/SEC."
850 PRINT "MACH NUMBER";M"ALTITUDE";Y"METER"
860 PRINT "VISCOSITY";M7"NEWTON-SEC./METER↑2"
890 PRINT "TRANSITION REYNOLD'S NUMBER";R1
910 PRINT "BODY SURFACE AREA";S3"METER↑2"
920 PRINT "PROJECTILE SURFACE AREA";S3"METER↑2"
930 PRINT "ITERATION CONSTANT";D1
940 PRINT "TRANSITION LENGTH,X*, IS";X"METER"
950 PRINT "SURFACE AREA WITH LAMINAR FLOW IS";S"METER↑2"
960 PRINT "SURFACE AREA WITH TURBULENT FLOW IS";S3-S
970 PRINT "REYNOLD'S NUMBER BASED ON TOTAL PROJECTILE LENGTH IS";R2
980 PRINT "LAMINAR SKIN FRICTION COEFFFICIENT IS";C1
990 PRINT "TURBULENT SKIN FRICTION COEFFICIENT IS";Q1
1000 PRINT "ITERATION CRITERIA IS";Q5
1010 PRINT "DYNAMIC PRESSURE IS";Q9"NEWTON/METER↑2"
1020 PRINT "DENSITY OF FREESTREAM IS";Z"KILOGRAM/METER↑3"
1030 PRINT ""
1040 PRINT "SKIN FRICTION DRAG IS";D7"NEWTONS"
1050 PRINT "SKIN FRICTION DRAG COEFFICIENT IS";C7
1060 PRINT ""
1170 PRINT "XXXXXXXXXXXXXXXXXXXXXXXXXXXXXXXXXXXXXXXXXXXXXXXXXXXXXXXXXXXXXXXXX
1180 STOP
1190 END
```

TABLE IV

HP 9830 PROGRAM TO CALCULATE BODY DRAG; SAMPLE OUTPUT

```
THIS PROGRAM CALCULATES PROJECTILE BODY DRAG.
THIS PROGRAM IA STORED IN FILE 0.


FOR SUPERSONIC VELOCITY INSERT 0.

****************************
ALTITUDE IS 0     METER

PROJECTILE LENGTH 1.5494  METER
PROJECTILE DIAMETER 0.12598    METER
BASE AREA 0.012465023   METER SQUARED
SPEED OF SOUND 340  VELOCITY OF PROJECTILE 1020    METER/SEC.
MACH NUMBER 3    ALTITUDE 0    METER
VISCOSITY 1.80000E-05   NEWTON-SEC./METER↑2
TRANSITION REYNOLD'S NUMBER 2000000
BODY SURFACE AREA 0.613218189   METER↑2
PROJECTILE SURFACE AREA 0.613218189   METER↑2
ITERATION CONSTANT 100
TRANSITION LENGTH,X*, IS 0.028811525   METER
SURFACE AREA WITH LAMINAR FLOW IS 0.011402963   METER↑2
SURFACE AREA WITH TURBULENT FLOW IS 0.601815226
REYNOLD'S NUMBER BASED ON TOTAL PROJECTILE LENGTH IS 107554183.3
LAMINAR SKIN FRICTION COEFFFICIENT IS 6.26412E-04
TURBULENT SKIN FRICTION COEFFICIENT IS 1.24907E-03
ITERATION CRITERIA IS 8.67261E-07
DYNAMIC PRESSURE IS 637245  NEWTON/METER↑2
DENSITY OF FREESTREAM IS 1.225   KILOGRAM/METER↑3

SKIN FRICTION DRAG IS 483.5749443   NEWTONS
SKIN FRICTION DRAG COEFFICIENT IS 0.060878545

XXXXXXXXXXXXXXXXXXXXXXXXXXXXXXXXXXXXXXXXXXXXXXXXXXXXXXXXXXXXXXXXXXXXXXXXXXXXXXXX
```

2. Tailfin Friction Drag Calculating the drag due to friction on the fins of Configuration I was very similar to the methodology in calculating the body drag due to friction. Figure 9 depicts the actual geometry. Table I provides the pertinent dimensions.

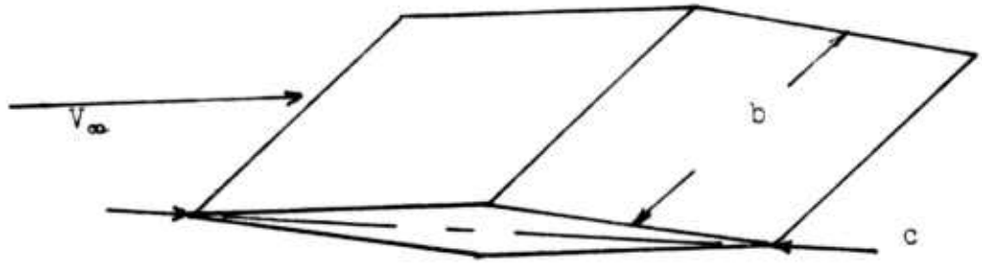

Figure 9. Tailfin geometry for Configuration I.

From the data, the surface area of each fin was calculated

$$A_s = 2bc = 0.012097 \text{ m}^2$$

The Reynolds number was calculated using the chord, c, the distance between the leading and trailing edges measured in the middle of the tailfin as the characteristic length

$$Re = \frac{\rho V c}{\mu} = 4.41 \times 10^6$$

Since the Reynolds number is greater than 2×10^6, the fin has both turbulent and laminar flow. Calculations were made to determine the coefficients of friction in both the turbulent and laminar regions. The location of transition was determined, and finally, the drag coefficient for each fin was calculated.

Using equations (12) through (21), the incompressible and compressible skin friction coefficients were evaluated for the fins. The results are

$C_{fi} = 0.003375$ and $C_{fc} = 0.002056$

in the turbulent region, and

$C_{fi} = 0.000939$ and $C_{fc} = 0.000626$

in the laminar region.

The location of transition was found to be at 0.453 chord by using the ratio of Re* to Re.

The surface area exposed to turbulent and laminar boundary layer flow conditions was determined using values of chord and span.

$A(x^*) = (0.453)(2)(c)(b) = 0.00548\ m^2$

$A(L) - A(x^*) = (0.547)(.0121) = 0.00662\ m^2$

Drag was calculated. Drag due to the laminar flow region was 2.18 N, and drag due to turbulent flow region was 8.67 N. The total drag per fin was 10.85 N. Finally, the drag coefficient was determined to be 0.0014 per fin based on fin area.

The above steps also were programmed for the HP 9830 computer. The program is listed in Table V with a sample program output in Table VI. By entering the velocity, span, chord and altitude, the skin friction drag can be calculated.

TABLE V

HP 9830 PROGRAM TO CALCULATE WING FRICTION DRAG; PROGRAM STEPS

```
10 PRINT "THIS PROGRAM CALCULATES WING FRICTION DRAG."
20 PRINT "THIS PROGRAM IS STORED IN FILE 2."
30 PRINT ""
40 DEG
50 D1=100
60 DISP "PRINT INPUT?YES=1 NO=0";
70 INPUT K
80 PRINT
90 PRINT "FOR SUPERSONIC VELOCITY INSERT 0."
100 PRINT
110 DISP "SEE PRINTED STATEMENT CONCERNING VELOCITY";
120 INPUT K9
130 D1=100
140 L=0.0635
150 B=0.09525
160 A=L*B
170 A1=340
180 V=680
190 M=V/A1
200 H=7620
210 Y=3000
220 PRINT "**************************"
230 PRINT "ALTITUDE IS";Y"METER"
240 R0=1.225
250 Z=R0*EXP(-Y/H)
260 M7=1.8E-05
270 R1=2E+06
280 X=(R1*M7*EXP(Y/H))/(R0*V)
292 IF K9=0 THEN 310
310 S3=2*L*B
320 IF L>X THEN 350
330 S=S3
340 GOTO 420
350 S=2*B*X
420 C1=1.328/(SQR(R1))
425 C1=C1/((1+0.45*M↑2)↑0.25)
430 R2=R1*(L/X)
440 PRINT "    "
450 Q1=C1
460 Q2=LGT(Q1*R2)
470 Q3=Q2↑2
480 Q4=0.058564/Q3
490 Q5=ABS(Q4-Q1)
500 IF Q5<1E-06 THEN 585
510 IF Q5<1E-05 THEN 570
520 IF Q5<1E-04 THEN 550
530 Q1=Q1+C1/D1
540 GOTO 460
550 Q1=Q1+C1/(5*D1)
```

TABLE V (CONTINUED)

```
560 GOTO 460
570 Q1=Q1+C1/(40*D1)
580 GOTO 460
585 Q1=Q1/((1+0.15*M↑2)↑0.58)
590 Q9=R0*(V↑2)*(0.5)*EXP(-Y/H)
600 D7=Q9*(C1*S+Q1*(S3-S))
610 C7=D7/(Q9*A)
670 IF K9=1 THEN 700
750 IF K=0 THEN 940
760 IF K9=1 THEN 790
780 GOTO 800
800 PRINT "WING CHORD LENGTH";L"METER"
810 PRINT "WING SPAN";B"METER"
830 PRINT "BACE AREA";A"METER SQUARED"
840 PRINT "SPEED OF SOUND";A1"VELOCITY OF PROJECTILE";V"METER/SEC."
850 PRINT "MACH NUMBER";M"ALTITUDE";Y"METER"
860 PRINT "VISCOSITY";M7"NEWTON-SEC./METER↑2"
890 PRINT "TRANSITION REYNOLD'S NUMBER";R1
910 PRINT "WING SURFACE AREA";S3"METER↑2"
930 PRINT "ITERATION CONSTANT";D1
940 PRINT "TRANSITION LENGTH,X*, IS";X"METER"
950 PRINT "SURFACE AREA WITH LAMINAR FLOW IS";S"METER↑2"
960 PRINT "SURFACE AREA WITH TURBULENT FLOW IS";S3-S
970 PRINT "REYNOLD'S NUMBER BASED ON TOTAL WING CHORD LENGTH IS";R2
980 PRINT "LAMINAR SKIN FRICTION COEFFFICIENT IS";C1
990 PRINT "TURBULENT SKIN FRICTION COEFFICIENT IS";Q1
1000 PRINT "ITERATION CRITERIA IS";Q5
1010 PRINT "DYNAMIC PRESSURE IS";Q9"NEWTON/METER↑2"
1020 PRINT "DENSITY OF FREESTREAM IS";Z"KILOGRAM/METER↑3"
1030 PRINT ""
1040 PRINT "SKIN FRICTION DRAG IS";D7"NEWTONS"
1050 PRINT "SKIN FRICTION DRAG COEFFICIENT IS";C7
1060 PRINT ""
1170 PRINT "XXXXXXXXXXXXXXXXXXXXXXXXXXXXXXXXXXXXXXXXXXXXXXXXXXXXXXXXXXXXXXX
1180 STOP
1190 END
```

TABLE VI

HP 9830 PROGRAM TO CALCULATE WING FRICTION DRAG; SAMPLE OUTPUT

```
THIS PROGRAM CALCULATES WING FRICTION DRAG.
THIS PROGRAM IS STORED IN FILE 2.


FOR SUPERSONIC VELOCITY INSERT 0.

**************************
ALTITUDE IS 3000    METER

WING CHORD LENGTH 0.0635  METER
WING SPAN 0.09525    METER
BASE AREA 6.04838E-03   METER SQUARED
SPEED OF SOUND 340  VELOCITY OF PROJECTILE 1020    METER/SEC.
MACH NUMBER 3    ALTITUDE 3000    METER
VISCOSITY 1.80000E-05   NEWTON-SEC./METER↑2
TRANSITION REYNOLD'S NUMBER 2000000
WING SURFACE AREA 0.01209675    METER↑2
ITERATION CONSTANT 100
TRANSITION LENGTH,X*, IS 0.042711844   METER
SURFACE AREA WITH LAMINAR FLOW IS 8.12661E-03   METER↑2
SURFACE AREA WITH TURBULENT FLOW IS 3.96014E-03
REYNOLD'S NUMBER BASED ON TOTAL WING CHORD LENGTH IS 2973414.132
LAMINAR SKIN FRICTION COEFFICIENT IS 6.26412E-04
TURBULENT SKIN FRICTION COEFFICIENT IS 2.19618E-03
ITERATION CRITERIA IS 8.57708E-07
DYNAMIC PRESSURE IS 429857.35  NEWTON/METER↑2
DENSITY OF FREESTREAM IS 0.826330931   KILOGRAM/METER↑3

SKIN FRICTION DRAG IS 5.929472164   NEWTONS
SKIN FRICTION DRAG COEFFICIENT IS 2.28062E-03

XXXXXXXX
```

3. Tailfin Wave Drag

Wave drag was calculated for the GLM tailfin. Calculations were made for double-wedge airfoils with the aerodynamic geometry as listed in Table I at several angles of attack and at several Mach numbers. Angles of attack between 0 and 15 degrees were analyzed for each airfoil. Mach numbers considered were 2.0, 2.5, and 3.0. The procedure for calculations of tailfin drag was discussed in Section F of the Aerodynamic Theory. Results are tabulated for each configuration in Section V.

4. Tailfin Lift Calculation

Lift was calculated for the GLM tailfin. Calculations were made utilizing the double-wedge airfoil discussed in Section G of the Aerodynamic Theory using the aerodynamic geometry listed in Table I for each fin. Methodology was similar to the approach for calculating wave drag for each fin. Equation (29) is the applicable equation discussed in the theory. Calculations were made for each fin at angles of attack between 5 and 15 degrees. Mach numbers considered were 2.0, 2.5, and 3.0. Results for all three configurations are included in the lift coefficients presented in Tables VIII, X, and XII in Section V.

5. Tailfin Placement and Packaging

Simultaneously with the calculations of fin drag and fin lift, fin placement and packaging on the configuration were analyzed. In addition, thickness ratio restrictions, fin deployment and storage were addressed.

Since the GLM configurations are fired from the 5"/54 MK 45 gun system, the problems of packaging and storage become apparent. A location on the body was needed to allow the fins to remain retracted during the gun firing and then be deployed upon exit from the muzzle.

In addition, since from the basic ground rules, the propulsion system was to be a ramjet, the geometry of the after body section of the missile was to be determined primarily by the size of the exhaust nozzle required for the ramjet to sustain Mach 3.0. Consequently, fin placement was bounded by the 5"/54 gun tube externally and the required exhaust nozzle size internally.

Several other parameters influenced final fin placement on Configuration I (and not coincidentally, the subsequent configurations).

Historically, the fin thickness ratio, that is the thickness to chord ratio, has been approximately 5 percent for most missile designs. For the tailfins of the GLM the wedge angle was 5^{o}. The thickness ratio was calculated to be over 8 percent. Because of the axial g-loading placed on the missile by the gun launch, this ratio was considered satisfactory and was not changed. In this thesis, a simple fin system was envisioned for the GLM. The simplicity was required for both the packaging of the tailfin system and the mechanism for tailfin deployment. Future study of the tailfin system is recommended.

Figures 10 and 11 show the location chosen for tailfin placement on the GLM. Figure 12 depicts the envisioned design of the hinge mechanism used to deploy the fins upon launch. The figures should be viewed as sketches only. For example, the inward tapering of the lines of the GLM aft body section in Figure 10 are envisioned only as a possible aid to keep the center of pressure aft during flight.

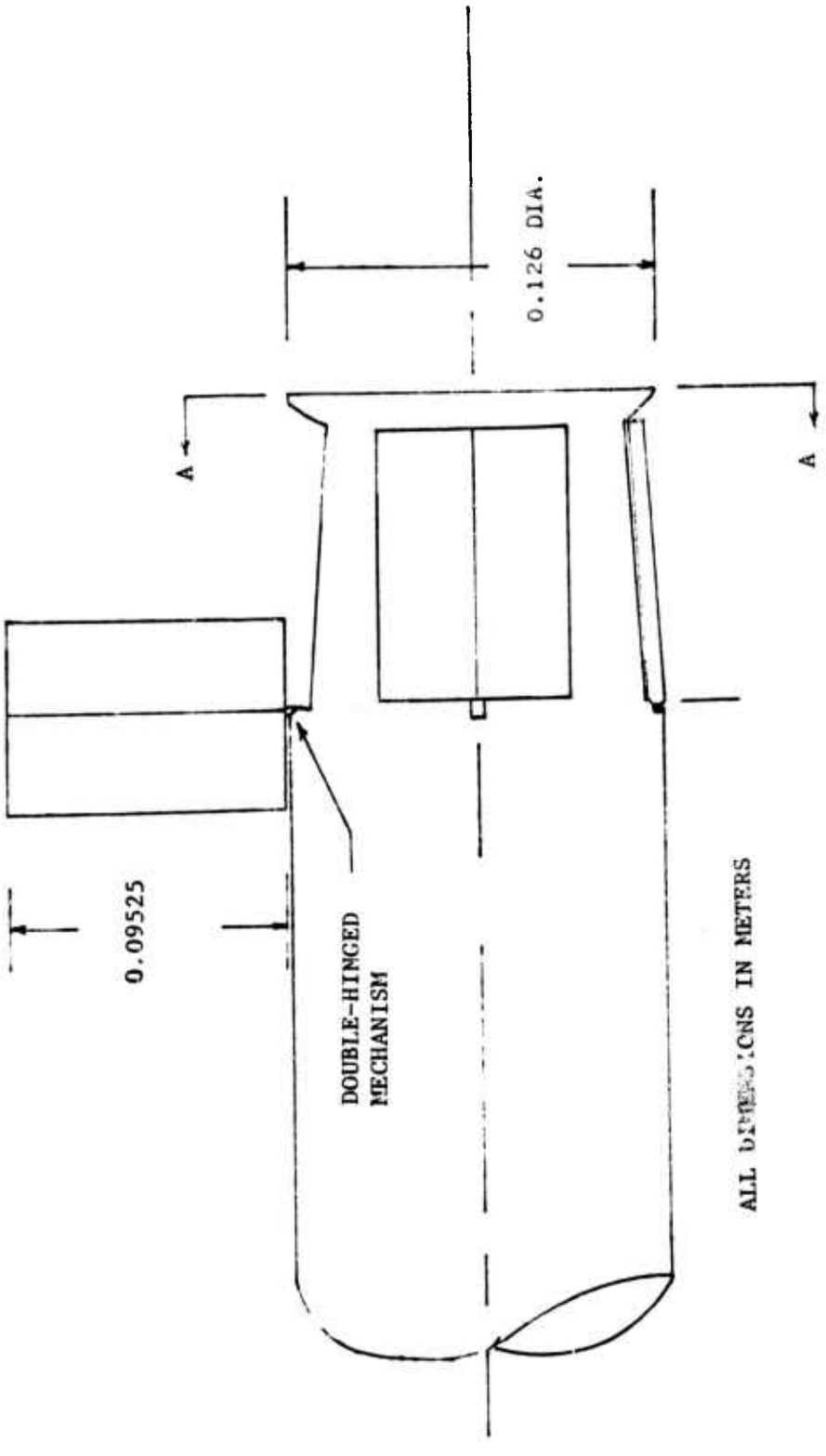

Figure 10. Aft Body Fin Design.

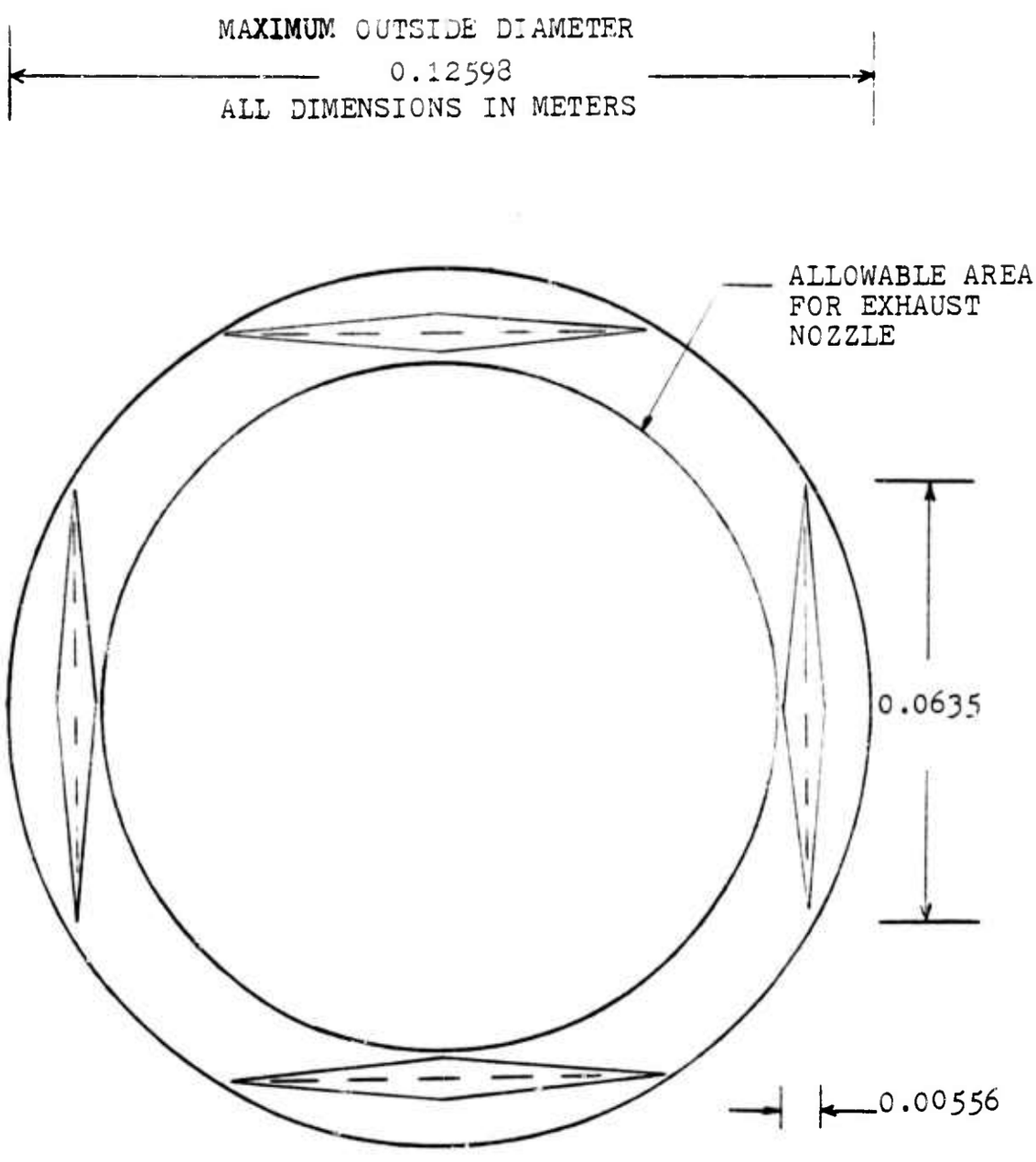

SECTION A - A

Figure 11. Aft Body Fin Design. Section A - A.

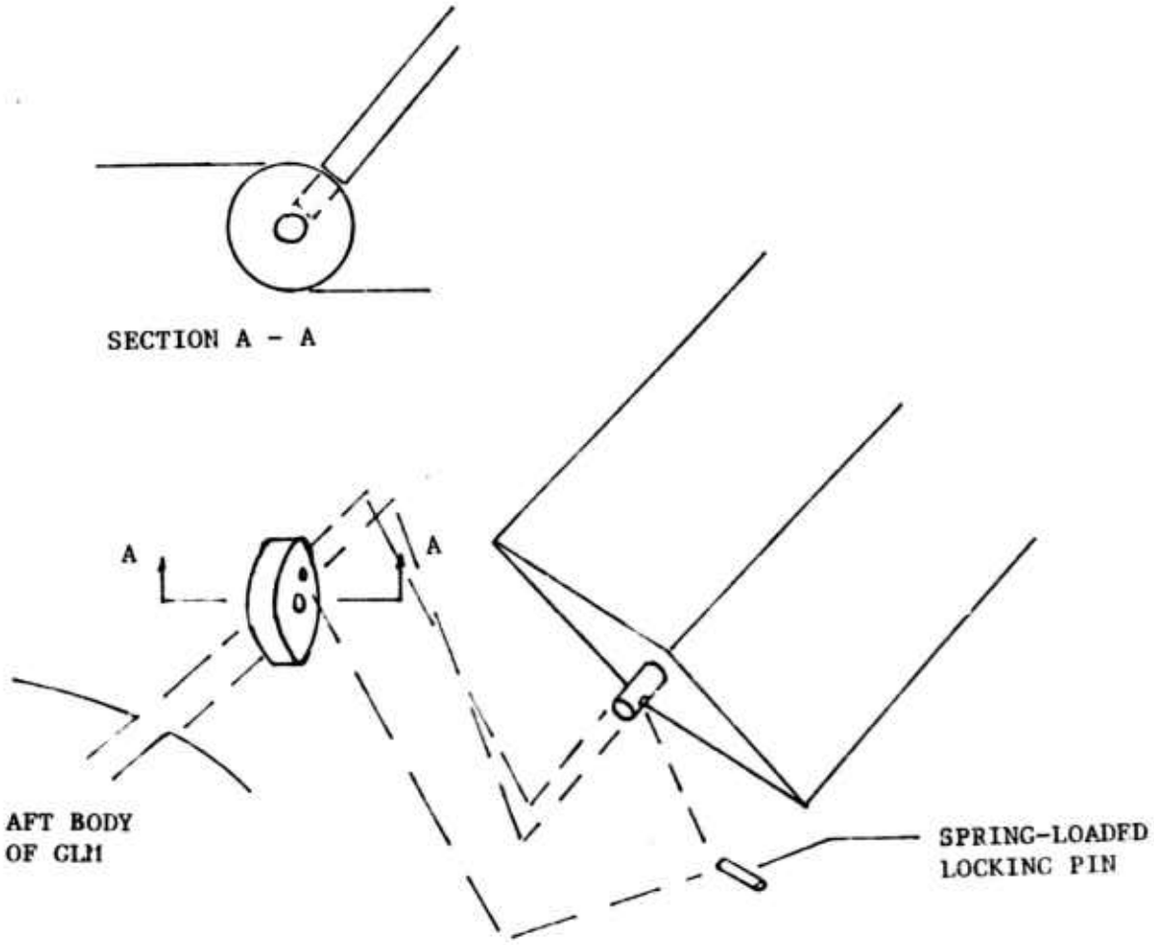

Figure 12. Fin Deployment Design for GLM.

6. Center of Pressure and Lift-to-Drag Ratio

Garnell and East [15] state that when considering the lifting forces on missiles it is convenient first of all to consider the combined normal forces due to incidence on the body and lifting surfaces as acting through a point on the body called the center of pressure. The center of pressure location when compared with the center of gravity location can be a good indicator of the stability of a flight vehicle. Calculation of the center of pressure c.p. location was conducted for the 5"/54 GLM.

In the calculation for the location of the center of pressure, the lift coefficient values for the nose (including the contribution by the necking), the body, and the tailfins were positioned on the configuration axis. Figure 13 illustrates the technique.

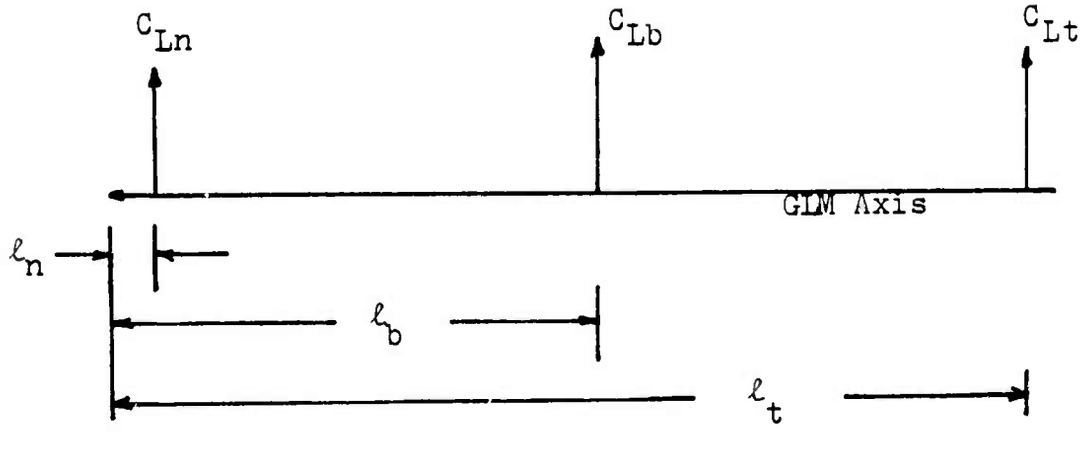

Figure 13. Location of lift coefficients on GLM axis.

The c.p. location was found by dividing the summation of the moment arms generated by individual components of the lift coefficient by the summation of the individual coefficients of lift.

$$\ell_{cp} = \frac{\ell_n C_{Ln} + \ell_b C_{Lb} + \ell_t C_{Lt}}{(C_{Ln} + C_{Lb} + C_{Lt})} \qquad (35)$$

After inserting values into equation (35), $\ell_{cp} = 0.6335$ m for Configuration I.

Lift-to-drag ratio is simply, L/D, the lift divided by the drag; the ratio also can be determined by C_L / C_D. For Configuration I at an angle of attack equal to 5^o, the value of L/D is 5.14 at Mach 3.0.

Figure 14 in Section V, shows Configuration I; which is the result of the analysis conducted in this section. In a similar fashion, the designs of Configurations II and III were calculated. The results also are shown.

V. AERODYNAMIC RESULTS

A. CONFIGURATION I

The initial aerodynamic design analyzed in this thesis was Configuration I. The major emphasis with Configuration I was that the inlet for the ramjet engine should utilize as much of the incoming volume of air as possible. Figure 14 depicts the aerodynamic configuration while Table VII provides the geometric characteristics and Table VIII provides the calculated aerodynamic data. Estimated lift and drag characteristics are functions of angle of attack, and the lift coefficient versus the drag coefficient is provided in Figures 15 through 17. In order to meet the loading system constraint specified in Section II, Configuration I was reduced in available length from 1.55 meters to 1.29 meters. Because of this reduction in length, significant missile volume was lost.

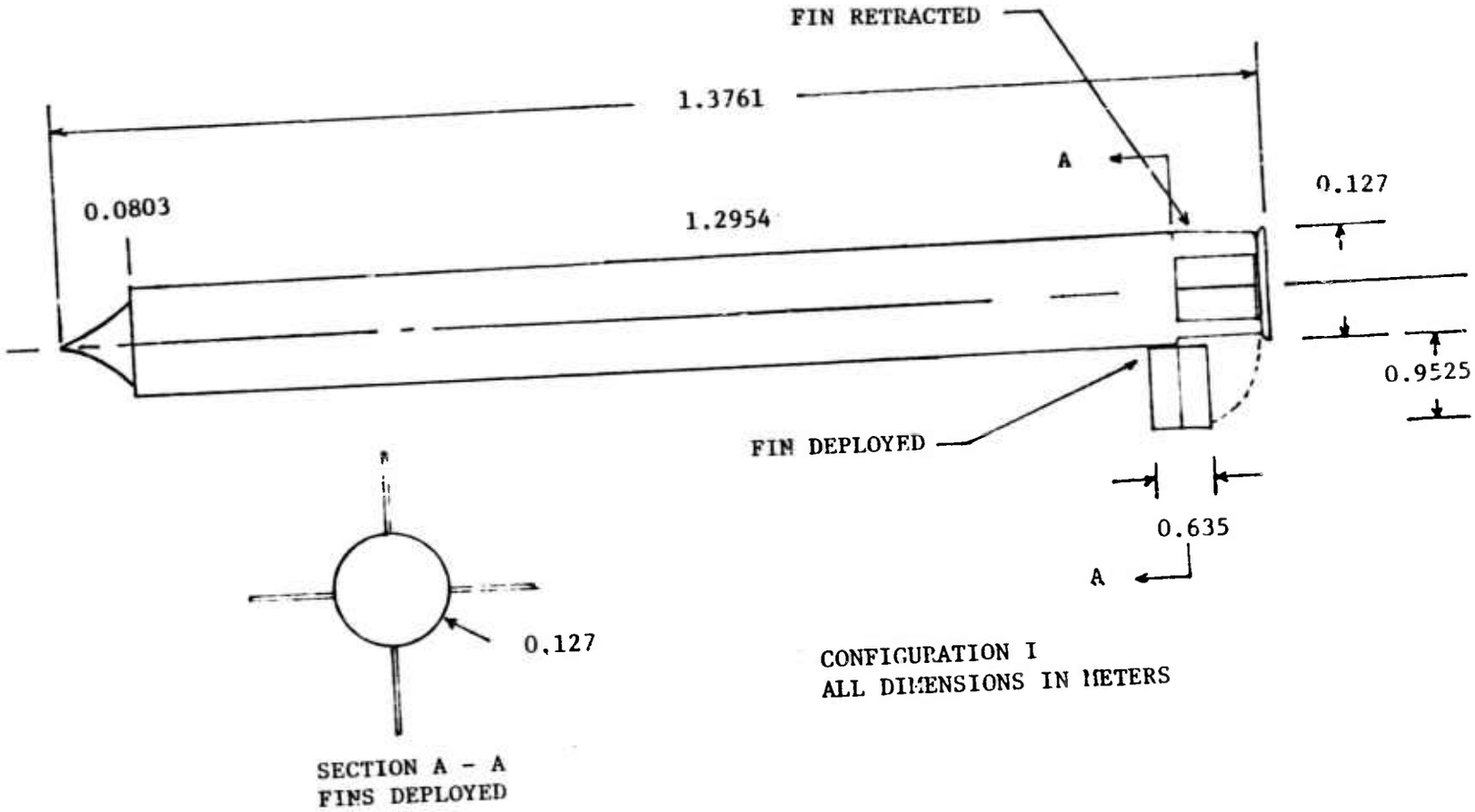

Figure 14. Configuration I.

TABLE VII

GEOMETRIC CHARACTERISTICS FOR GEOMETRIC CONFIGURATION I

BODY:	
Length, overall, m.	1.3716
Length, forebody, m.	0
Diameter, overall, m.	0.1270
Volume, m^3	0.0164
Wetted area, m^2	0.5168
Base area, m^2	0.0127
Cone angle of forebody, deg	0
TAILFIN:	
Area (2 panels), m^2	0.01210
Chord, m.	0.0635
Span, m.	0.09525
Thickness ratio	0.0875
Aspect ratio	1.499

TABLE VIII

AERODYNAMIC DATA FOR GLM CONFIGURATION I

Mach No.	2.0	2.5	3.0	(α) deg
C_D	0.146	0.122	0.105	0
C_D	0.164	0.135	0.115	5
C_D	0.217	0.175	0.148	10
C_D	0.305	0.242	0.202	15

LIFT COEFFICIENTS:

Mach No.	2.0	2.5	3.0
α = 5			
C_{L_N}	0.175	0.175	0.175
C_{L_B}	0.293	0.293	0.293
C_{L_T}	0.164	0.150	0.123
C_L	0.632	0.618	0.591
α = 10			
C_{L_N}	0.349	0.349	0.349
C_{L_B}	0.824	0.824	0.824
C_{L_T}	0.279	0.209	0.183
C_L	1.452	1.382	1.371

TABLE VIII (CONTINUED)

AERODYNAMIC DATA FOR GLM CONFIGURATION I

LIFT COEFFICIENTS:			
Mach No.	2.0	2.5	3.0
α = 15			
C_{L_N}	0.524	0.524	0.524
C_{L_B}	1.592	1.592	1.592
C_{L_T}	0.424	0.301	0.280
C_L	2.540	2.416	2.395

Lift-to-drag ratio at α = 5 degrees ---------- 5.14

Center of pressure, m., as measured from nose tip

at Mach 2.0 ---------- 0.634

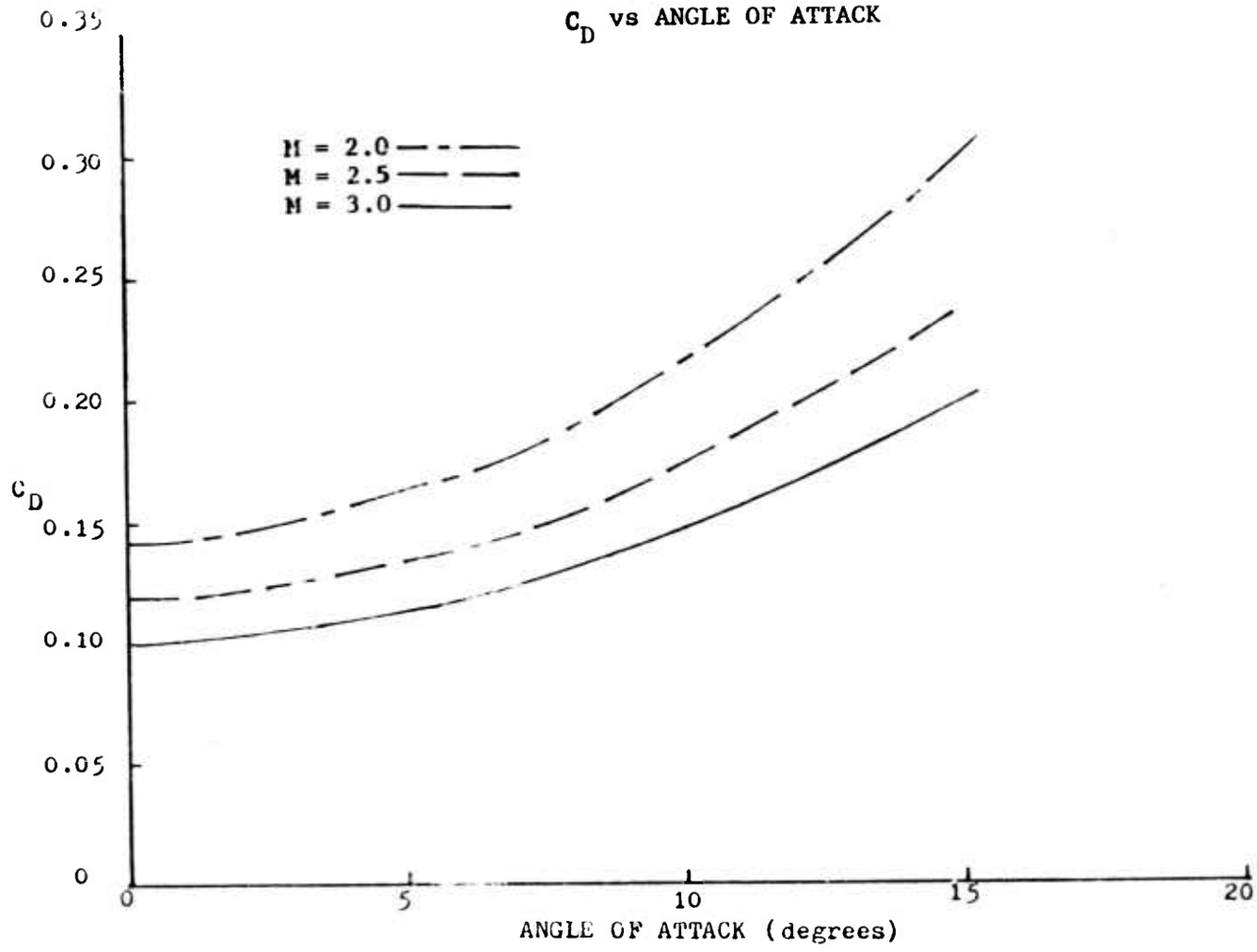

Figure 15. Coefficient of Drag versus angle of attack for Configuration I.

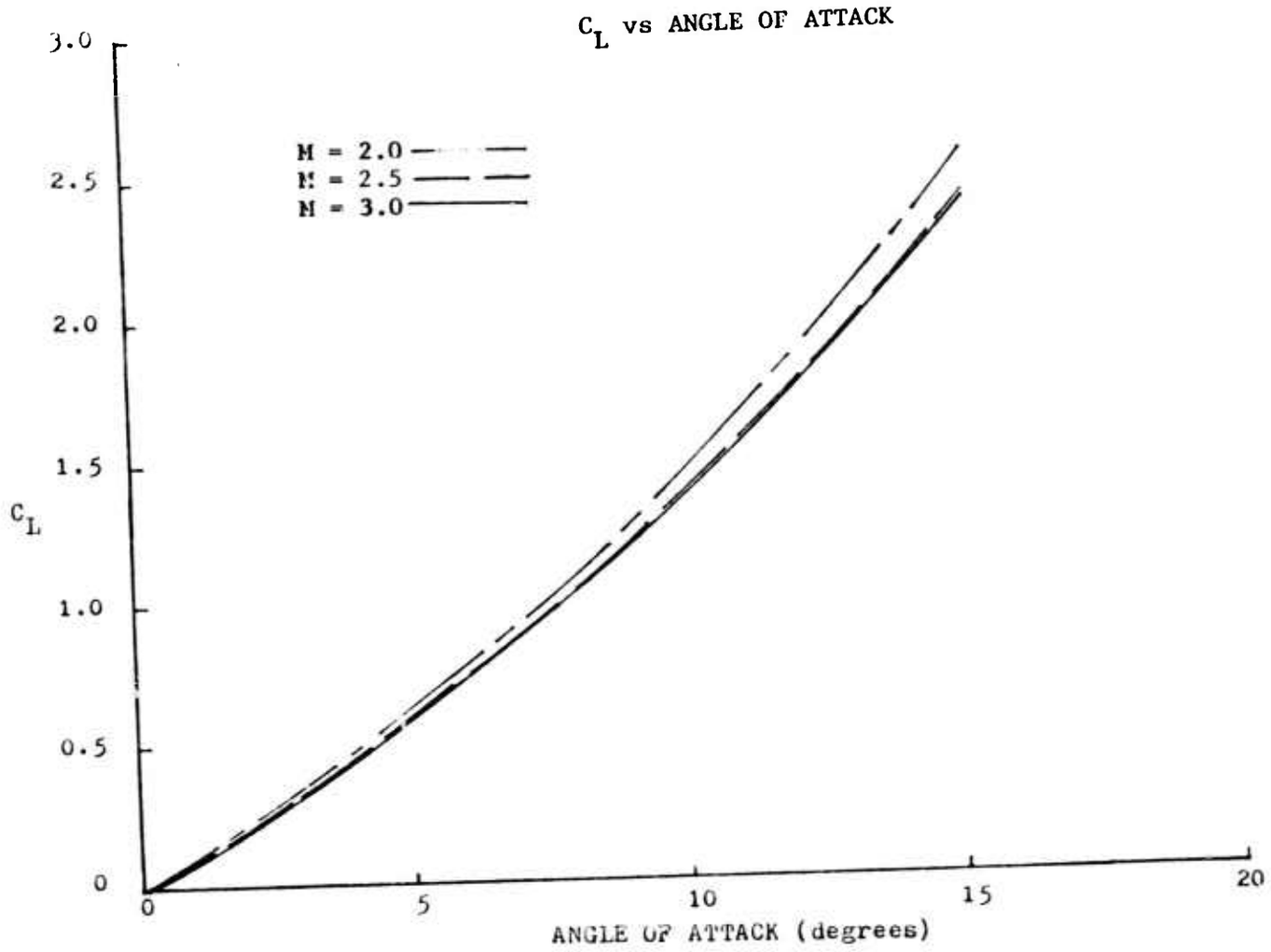

Figure 16. Coefficient of Lift versus angle of attack for Configuration I.

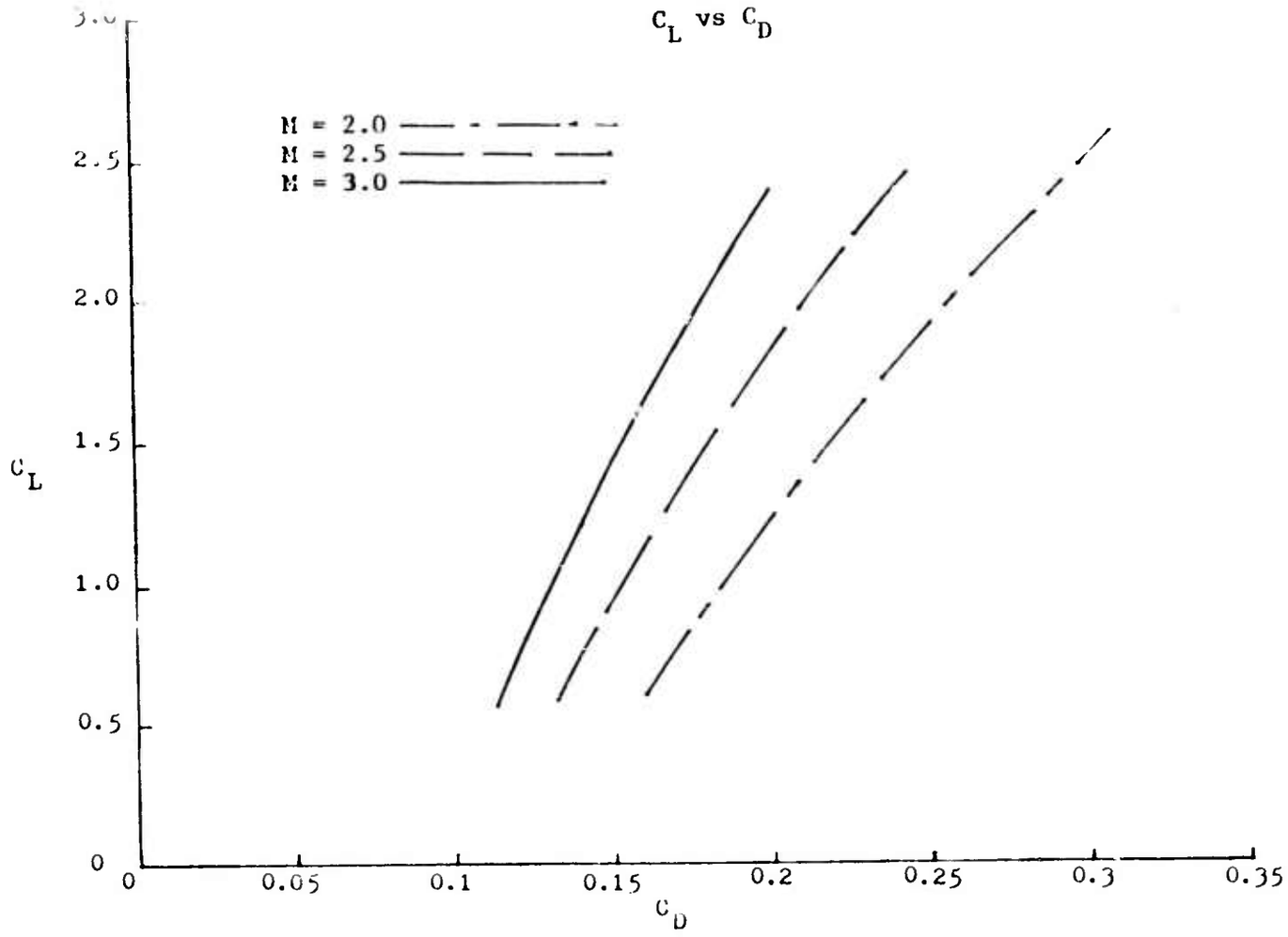

Figure 17. Coefficient of Lift versus Coefficient of Drag for Configuration I.

B. CONFIGURATION II

Configuration II was the second aerodynamic design analyzed in this thesis. A result of the 5"/54 Mk 45 gun loading system constraint, the configuration was a compromise attempt to maintain the lowest possible nose drag on the flight vehicle while maximizing the volume of the GLM. Figure 18 depicts the configuration.

The "bottleneck" forebody was designed to meet the specific constraint of the loading system to preclude any system modification. The geometric characteristics are presented in Table IX, and the aerodynamic data are provided in Table X. The gain in overall volume from Configuration I to Configuration II is slightly greater than 5 percent. Lift-to-drag ratio was decreased from Configuration I.

Estimated lift and drag coefficients as functions of angle of attack are presented in Figures 19 and 20. The lift coefficient versus the drag coefficient is depicted in Figure 21.

During analysis of Configuration II, a decision was made to modify the nose inlet configuration. This was based on the ramjet propulsion requirements in the companion thesis of Brown [4].

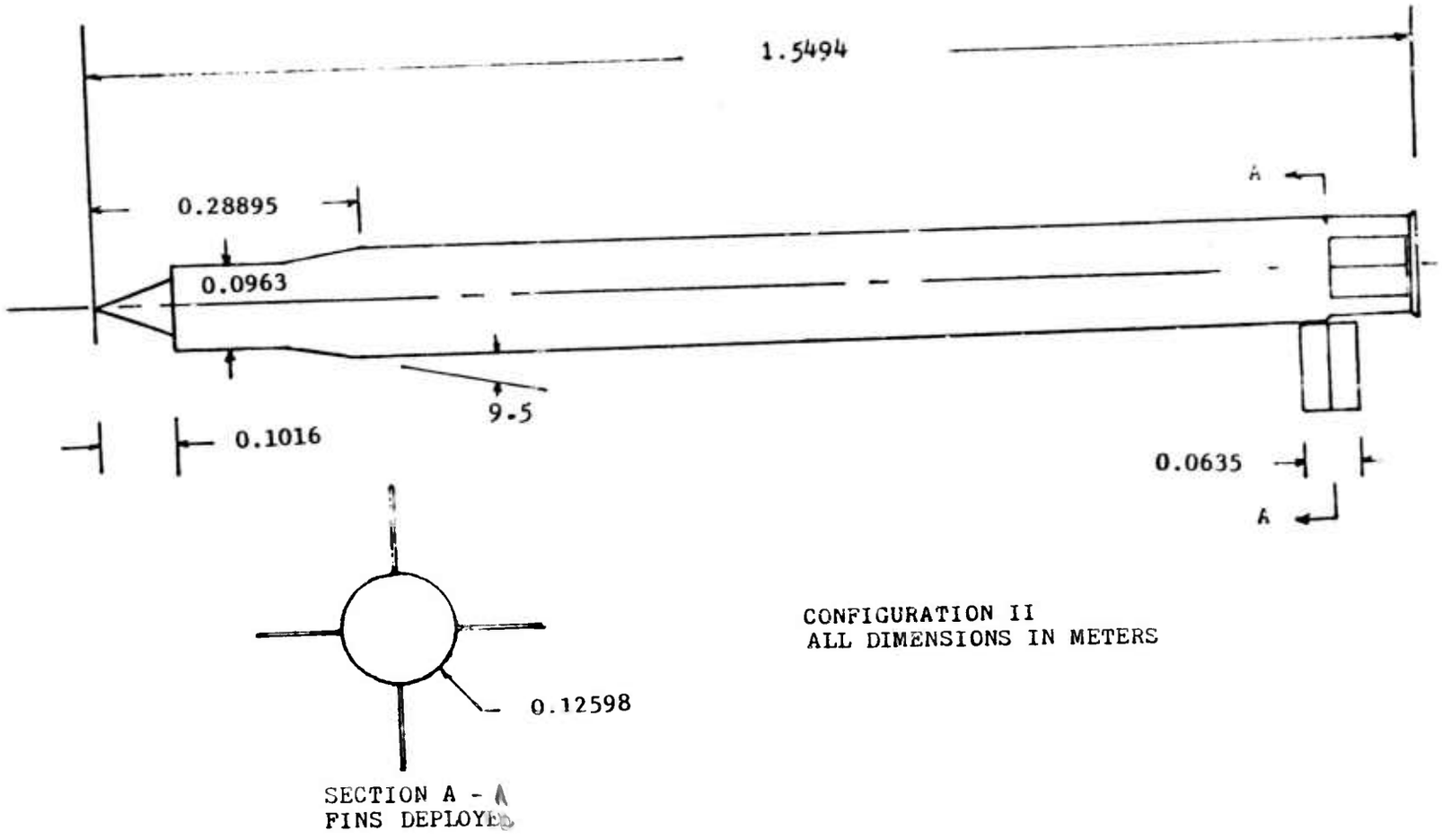

Figure 18. Configuration II.

TABLE IX

GEOMETRIC CHARACTERISTICS FOR GLM CONFIGURATION II

BODY:	
Length, overall, m.	1.5494
Length, forebody, m.	0.2889
Diameter, overall, m.	0.1259
Volume, m^3	0.0173
Wetted area, m^2	0.6132
Base area, m^2	0.0125
Cone angle of forebody, deg	9.5
TAILFIN:	
Area (2 panels), m^2	0.0121
Chord, m.	0.0635
Span, m.	0.0952
Thickness ratio	0.0875
Aspect ratio	1.499

TABLE X

AERODYNAMIC DATA FOR GLM CONFIGURATION II

Mach No.	2.0	2.5	3.0	(α) deg
C_{D_O}	0.411	0.330	0.277	0
C_D	0.428	0.343	0.288	5
C_D	0.481	0.383	0.320	10
C_D	0.569	0.449	0.374	15

LIFT COEFFICIENTS:

Mach No.	2.0	2.5	3.0
α = 5			
C_{L_N}	0.175	0.175	0.175
C_{L_B}	0.523	0.473	0.472
C_{L_T}	0.164	0.150	0.123
C_L	0.862	0.798	0.770
α = 10			
C_{L_N}	0.349	0.349	0.349
C_{L_B}	0.824	0.824	0.824
C_{L_T}	0.279	0.210	0.183
C_L	0.452	0.383	1.356

TABLE X (CONTINUED)

AERODYNAMIC DATA FOR GLM CONFIGURATION II

LIFT COEFFICIENTS:			
Mach No.	2.0	2.5	3.0
α = 15			
C_{L_N}	0.524	0.524	0.524
C_{L_B}	1.592	1.592	1.592
C_{L_T}	0.424	0.301	0.280
C_L	2.540	2.417	2.396

Lift-to-drag ratio at α = 5 degrees	2.67
Center of pressure, m., as measured from nose tip at Mach 2.0	0.839

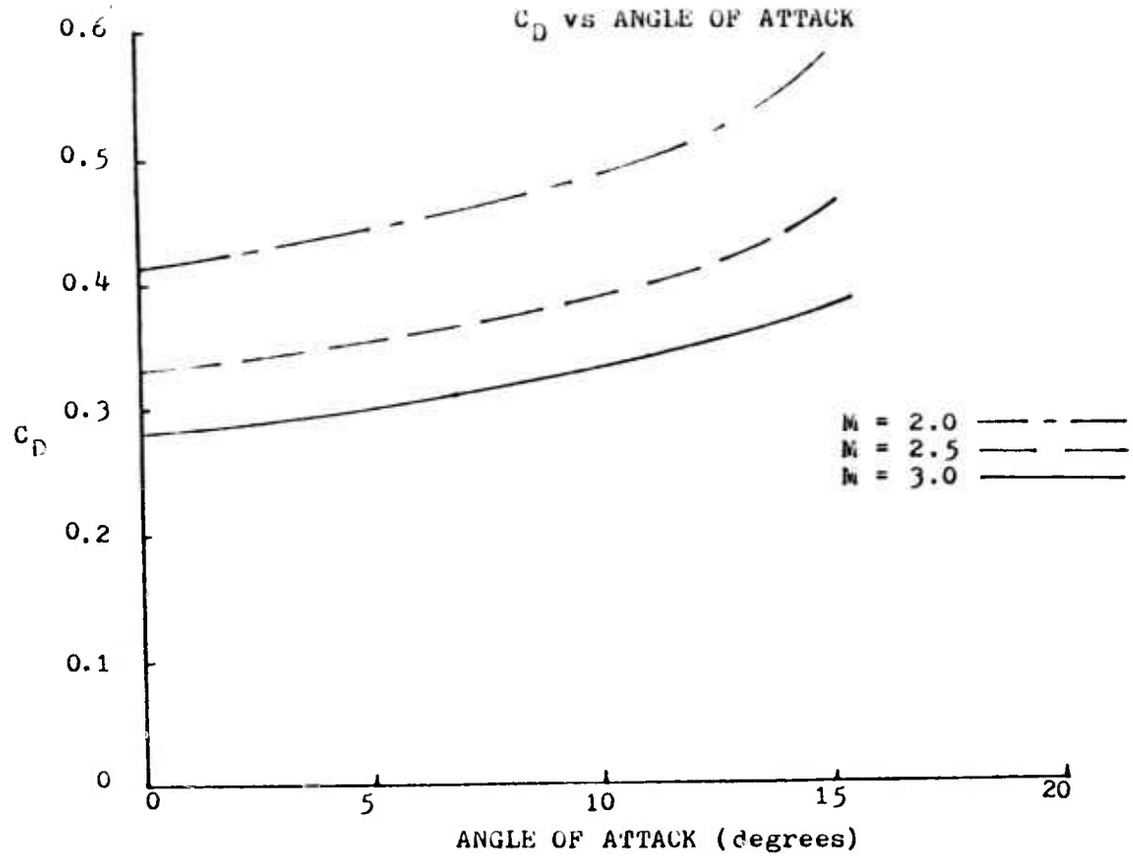

Figure 19. Coefficient of Drag versus angle of attack for Configuration II.

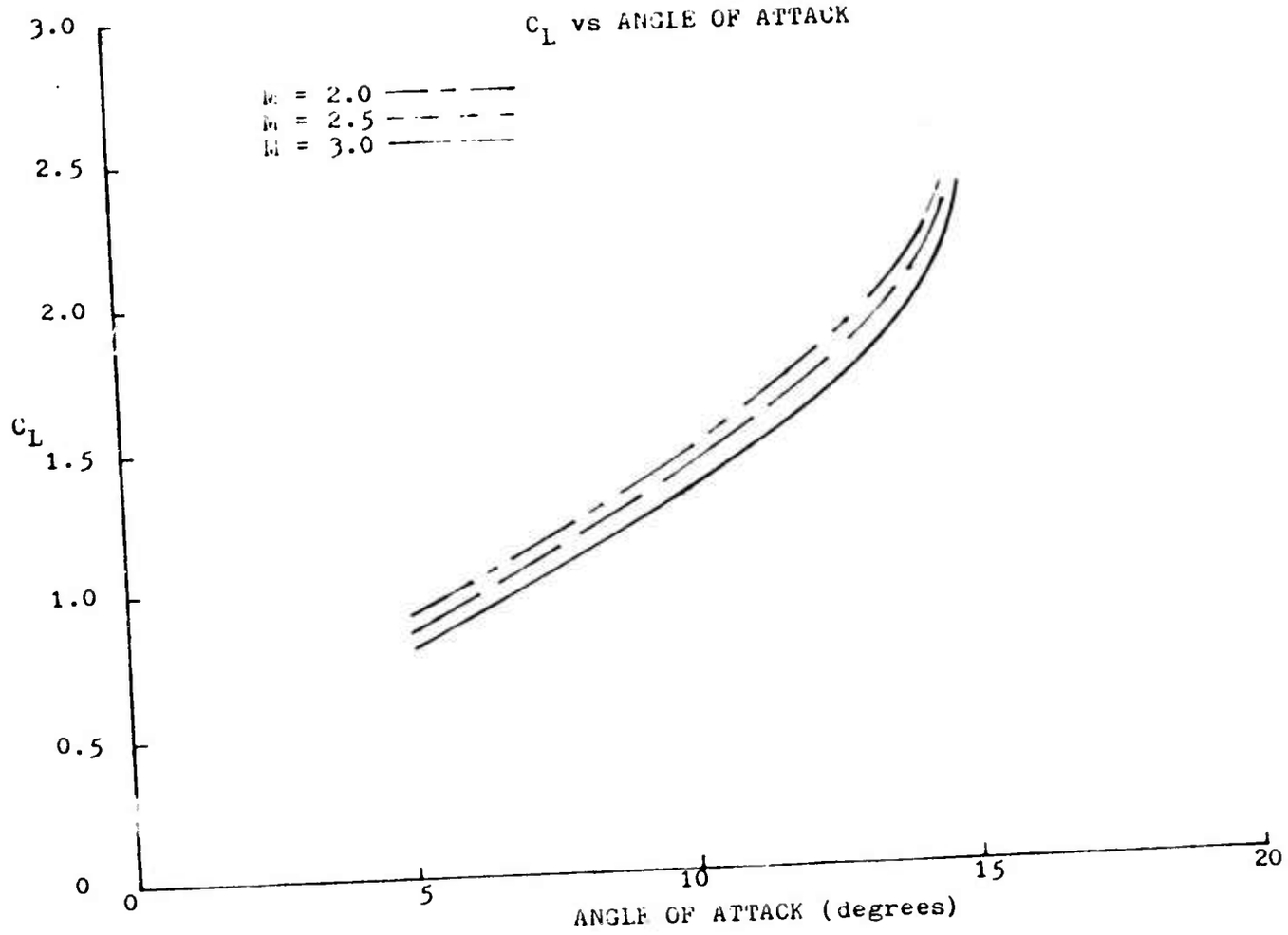

Figure 20. Coefficient of Lift versus angle of attack for Configuration II.

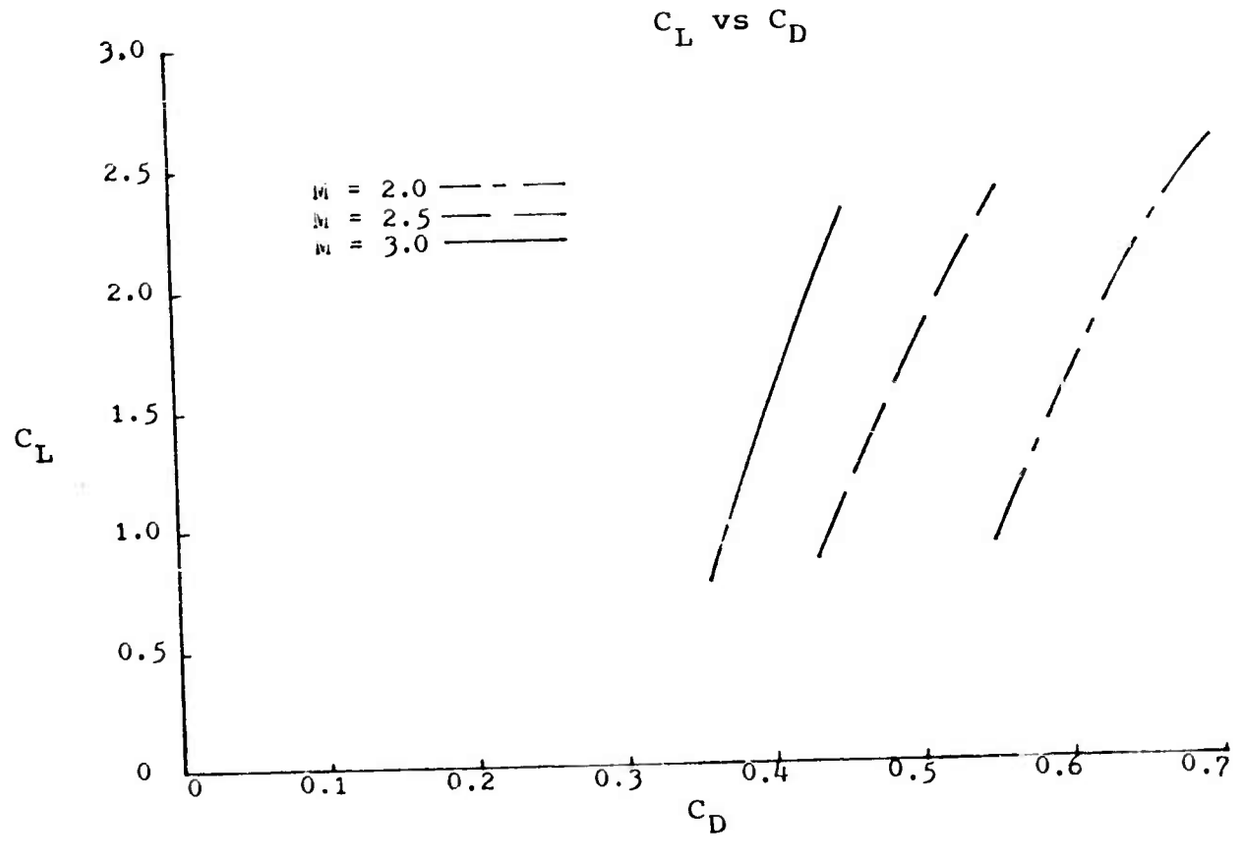

Figure 21. Coefficient of Lift versus Coefficient of Drag for Configuration II.

C. CONFIGURATION III

Configuration III was the result of the second significant compromise attempted in the thesis. As mentioned previously, the nose inlet geometry of Configurations I and II was not satisfactory for the ramjet engine. Too much air was entering the combustion chamber. Configuration III was the result of the modification to the nose inlet to reduce air intake. Figure 22 depicts the aerodynamic configuration in its entirety. While ensuring that the propulsion requirement was met satisfactorily, care was taken to ensure previously mentioned external geometric constraints still were being met. Figure 23 depicts the Configuration III forebody and the gun loading system constraint. Also depicted in Figure 23 is the estimated volume for the nose cap necessary to protect the nose inlet for the missile. The resultant loss of volume in Configuration III through modification of the nose geometry of Configuration II was considered insignificant.

The geometric characteristics for Configuration III are presented in Table XI. Table XII provides the pertinent aerodynamic data.

Estimated lift and drag coefficients as functions of angle of attack are presented in Figures 24 and 25. The lift coefficient versus the drag coefficient for Configuration III is depicted in Figure 26. Lift-to-drag ratio was decreased from Configuration II.

The center of pressure location defined in Section IV was calculated for all three configurations. The Configuration III c.p. location was compared with the center of gravity location presented in the companion thesis by Frazier [3]. Center of pressure location, as measured from the tip of the GLM nose, was 0.0464 meters aft of the center of gravity location measured from the same point. Both calculations assumed GLM launch at Mach 2.0.

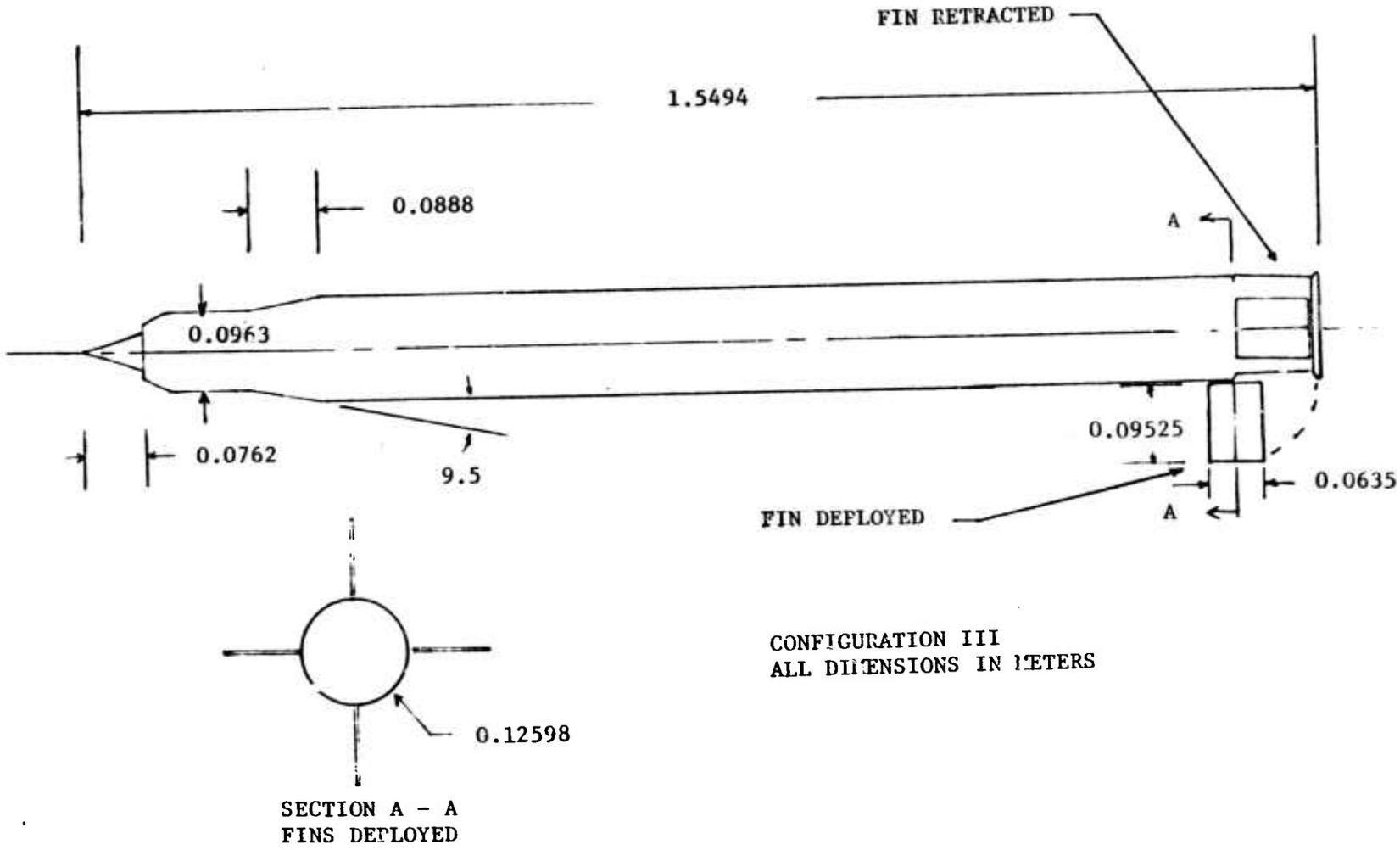

Figure 22. Configuration III.

TABLE XI

GEOMETRIC CHARACTERISTICS FOR GLM CONFIGURATION III

BODY:	
Length, overall, m.	1.5494
Length, forebody, m.	0.2889
Diameter, overall, m.	0.1259
Volume, m^3	0.01602
Wetted area, m^2	0.6132
Base area, m^2	0.0125
Cone angle of forebody, deg	9.5
TAILFIN:	
Area (2 panels), m^2	0.0121
Chord, m.	0.0635
Span, m.	0.0952
Thickness ratio	0.0875
Aspect ratio	0.499

TABLE XII

AERODYNAMIC DATA FOR GLM CONFIGURATION III

Mach No.	2.0	2.5	3.0	(α) deg
C_{D_O}	0.529	0.422	0.349	0
C_D	0.547	0.436	0.361	5
C_D	0.599	0.477	0.393	10
C_D	0.687	0.542	0.447	15

LIFT COEFFICIENTS:

Mach No.	2.0	2.5	3.0
α = 5			
C_{L_N}	0.175	0.175	0.175
C_{L_B}	0.523	0.473	0.472
C_{L_T}	0.164	0.510	0.123
C_L	0.862	0 798	0.770
α = 10			
C_{L_N}	0.349	0.349	0.349
C_{L_B}	0.824	0.824	0.824
C_{L_T}	0.279	0.210	0.183
C_L	1.452	1.382	1.371

TABLE XII

AERODYNAMIC DATA FOR GLM CONFIGURATION III

LIFT COEFFICIENTS:

Mach No.	2.0	2.5	3.0
α = 15			
C_{L_N}	0.524	0.524	0.524
C_{L_B}	1.592	1.592	1.592
C_{L_T}	0.424	0.301	0.280
C_L	2.540	2.417	2.359

Lift-to-drag ratio at α = 5 degrees ---------- 2.39

Center of pressure, m., as measured from nose tip

at Mach 2.0 ---------- 0.825

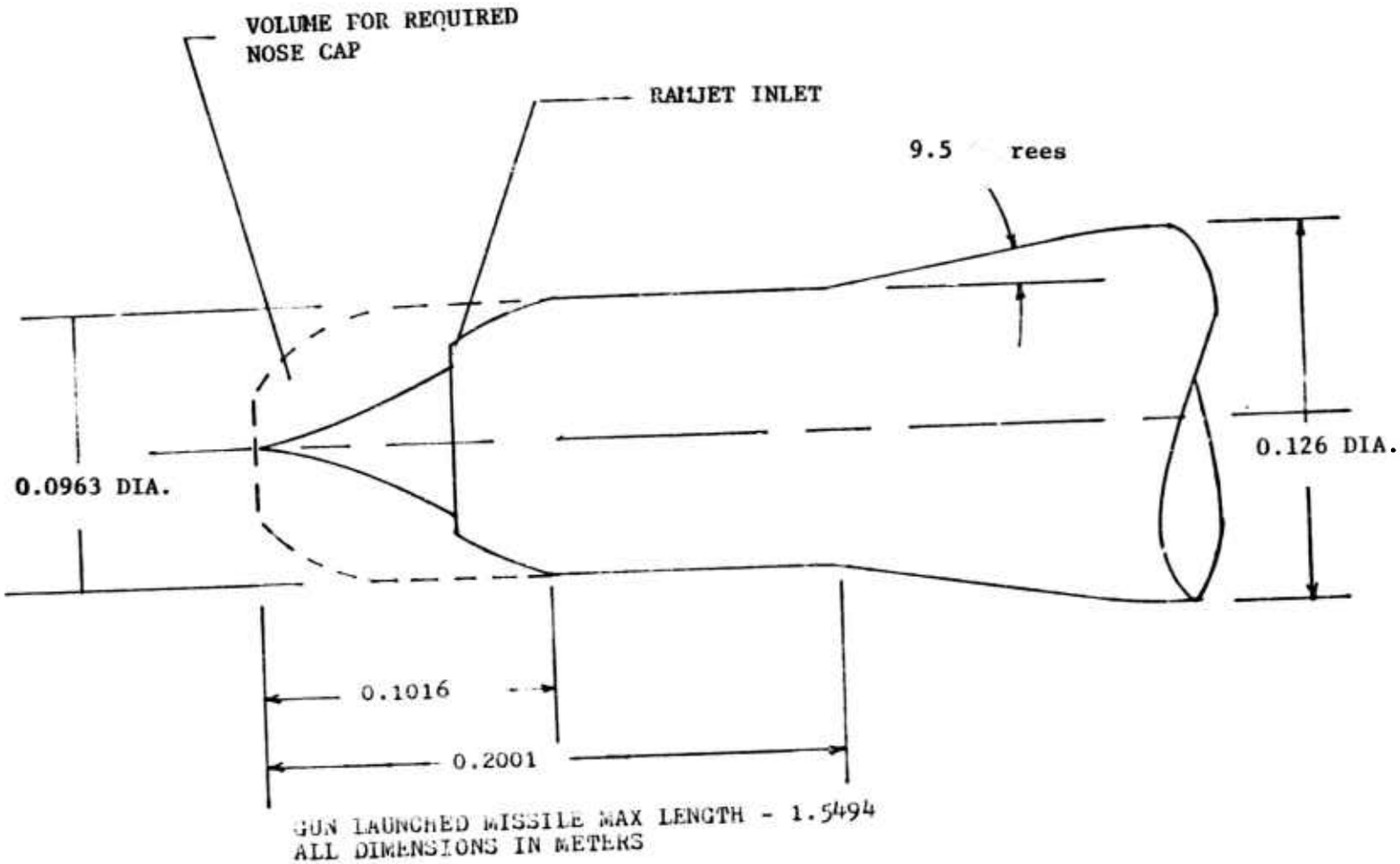

Figure 23. MK 45 Compatible Nose Shape.

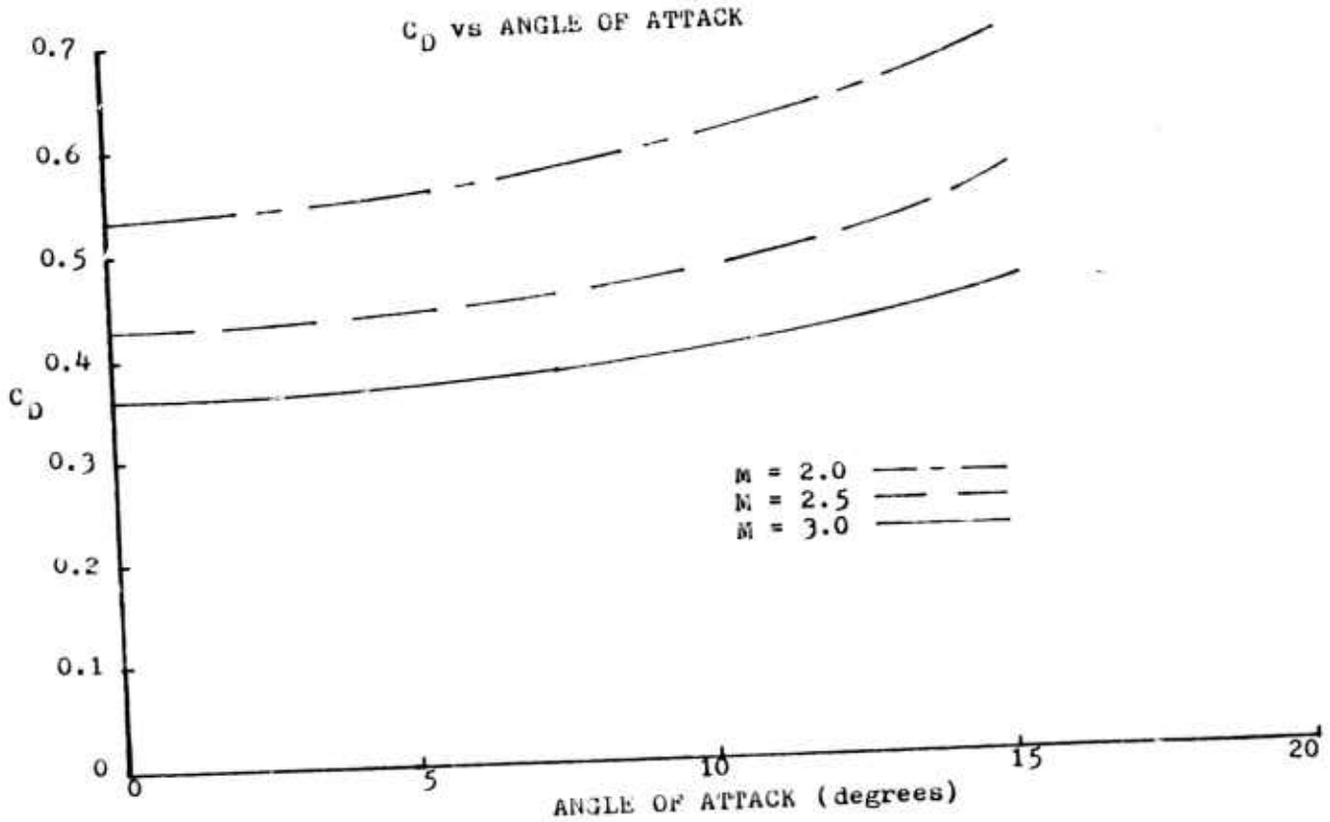

Figure 24. Coefficient of Drag versus angle of attack for Configuration III.

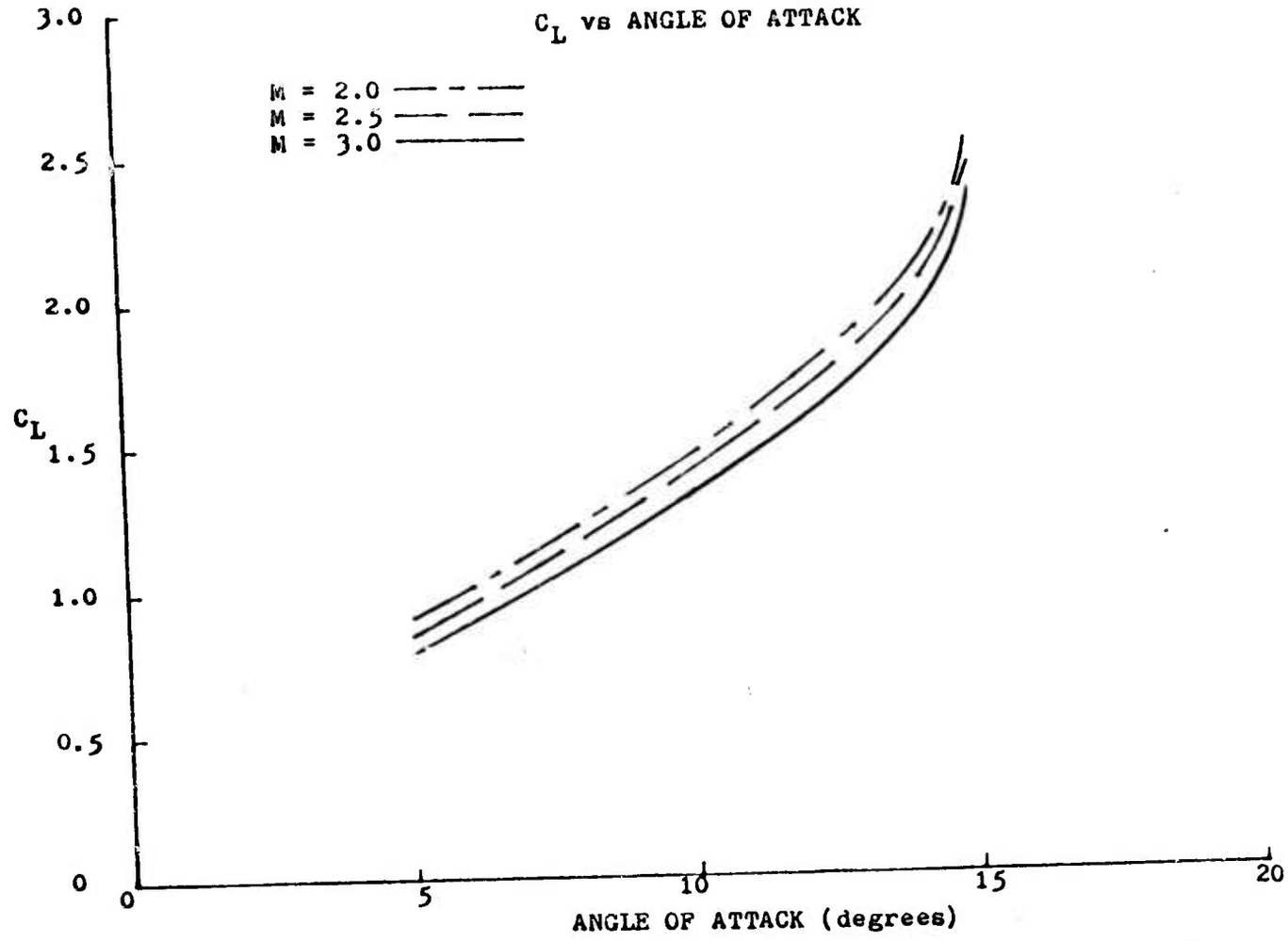

Figure 25. Coefficient of Lift versus angle of attack for Configuration III.

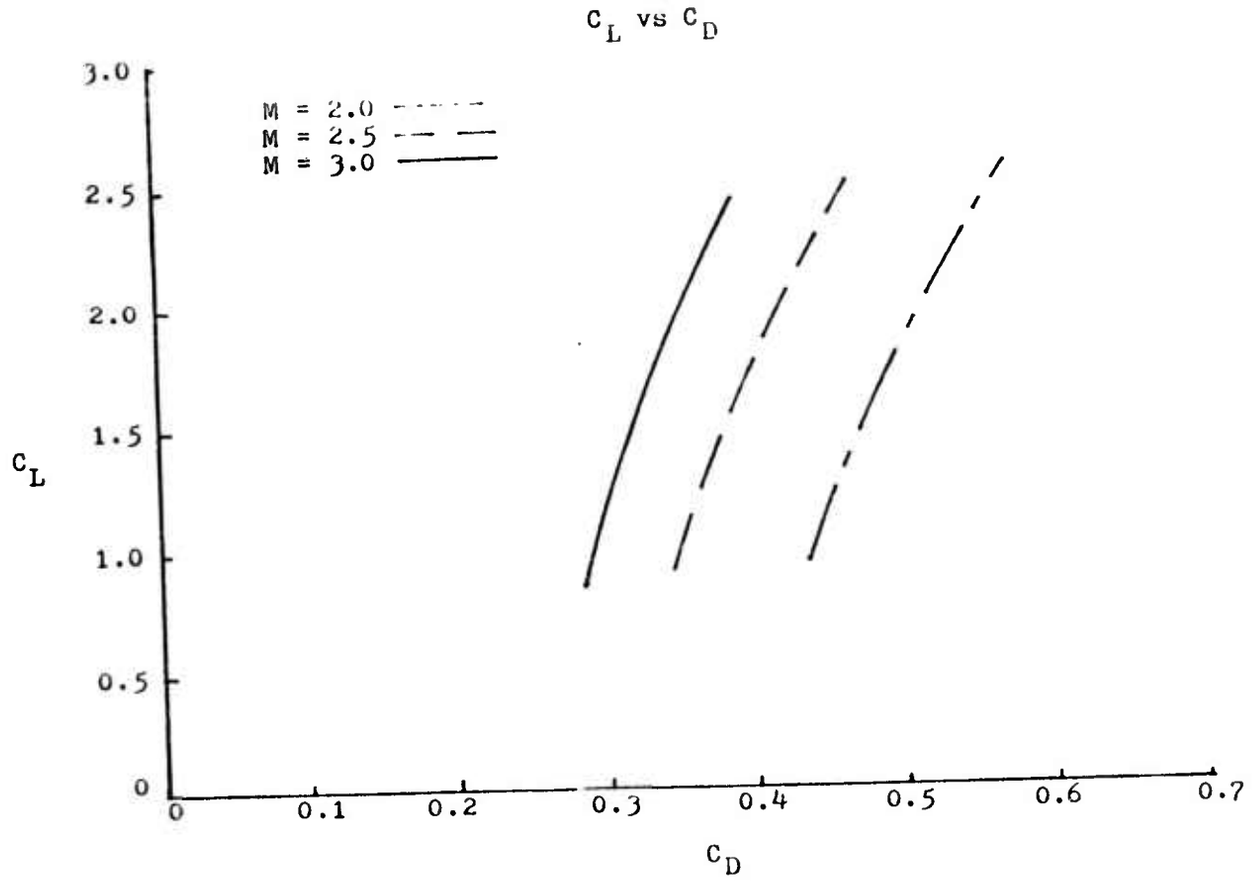

Figure 26. Coefficient of Lift versus Coefficient of Drag for Configuration III.

VI. REACTION JET CONTROL THEORY

A. BACKGROUND

Reaction jet control technology received significant impetus in 1964 when, in a series of wind tunnel experiments, Zukoski and Spaid [16] conducted a study of the flow field around an injection port for secondary injection of a gas normal to the supersonic stream. From their data, they were able to calculate a scale parameter that correlated the data quite well. In their analytical model, Zukoski and Spaid likened the resultant shock pattern from the secondary injection to that produced by blunt axisymmetric bodies. For the experiment, the underexpanded jet flow was sonic at the injector, with additional expansion through a strong Prandtl-Meyer expansion fan. Wall boundaries restricted the expansion of the flow out of the circular orifice. In 1968, the data bank was expanded by Zukoski and Spaid [17] when they investigated the interaction of the jet and freestream flows from transverse slots.

Within the next few years, others[18, 19, 20] followed in the investigations altering the parameters believed to have an effect on the freestream flow.

In early 1970, Wu [21] presented a two-dimensional analytical model of the resulting force normal to the freestream flow. The jet was considered to be equivalent to

a solid body interrupting the freestream flow.

Later that year, Nunn [22] presented a method for estimating the extent and shape of the three-dimensional flow field for a sonic jet exhausting normal to the supersonic freestream. The study was the first to address the problem of jet interaction on bodies of revolution.

Shortly thereafter, Grunnet [23] found that existing data suggested that effective blockage of the equivalent flow body (two-dimensional) was proportional to the injectant total pressure times the area of injection port flow regardless of the injectant or freestream gas properties. In addition, regardless of the given freestream conditions and the injector port shape, the relative interaction force was higher when the gas was injected at an angle upstream in the freestream flow. The total side force reached a maximum with the jet angled about 30 degrees upstream.

The interest in jet reaction control was increased since the early experiments seemed to confirm the belief that under certain conditions the side force produced by the control jet was greater than the thrust of the jet alone by some "amplification" factor. Accurate determination of the amplification of the jet control force resulting from aerodynamic interactions between the boundary layer and the flow field over the vehicle associated with the control jet is the problem. Inaccuracy is due to the presence of nonlinear phenomena associated with the mechanics of the interaction; notably boundary layer separation, viscous mixing,

the shock-wave boundary layer interaction, and a "Mach disk" associated with underexpanded jets. Thus, only simplified models for predicting approximations of the control forces have been developed.

Define a Cartesian coordinate system with coordinates x,y,z. The wall lies in the x-z plane. The freestream flow is in the x-direction, and the jet flow has velocity mainly in the y-direction. The nozzle is a slot which extends in the z-direction. In a study conducted for the Navy by Levine [24], the two-dimensional jet interaction flows using the coordinate system discussed above were evaluated. Scaling parameters were developed. In contrast to three-dimensional jet interaction such as would occur with a circular nozzle, the high pressure zones in the vicinity of the slot nozzle are constrained laterally. The pressure distribution on the wall is not a function of z. In the case of the GLM, the z-direction corresponds to a circumferential dimension of the body. The reaction jet control system envisioned for the 5"/54 GLM was based on two-dimensional jet reaction flow geometry.

B. DESIGN THEORY

For the preliminary design of the reaction jet control system of the 5"/54 GLM, the theory described in the Levine study [24] was used. The following assumptions and ground rules applicable to the reaction jet were considered to be integral to that study.

1. In order to simulate two-dimensional flow mentioned previously and thus achieve the greatest amplification of the thrust into a resultant side force, the injection slots for the reaction jets should be interdigitated between the GLM fins.

2. The jet is underexpanded and slightly supersonic.

3. The reaction jet control slots are angled 30 degrees upstream in the freestream flow.

4. The "amplification" factor K was defined:

$$K = \frac{F_t}{F_j}$$

where F_t is the total measured normal force due to the jet thrust plus the aerodynamic interaction, and F_j is the calculated jet thrust.

5. The characteristics of the two-dimensional jet interaction flow field are depicted in Figure 27 with an indication of the associated induced pressure field.

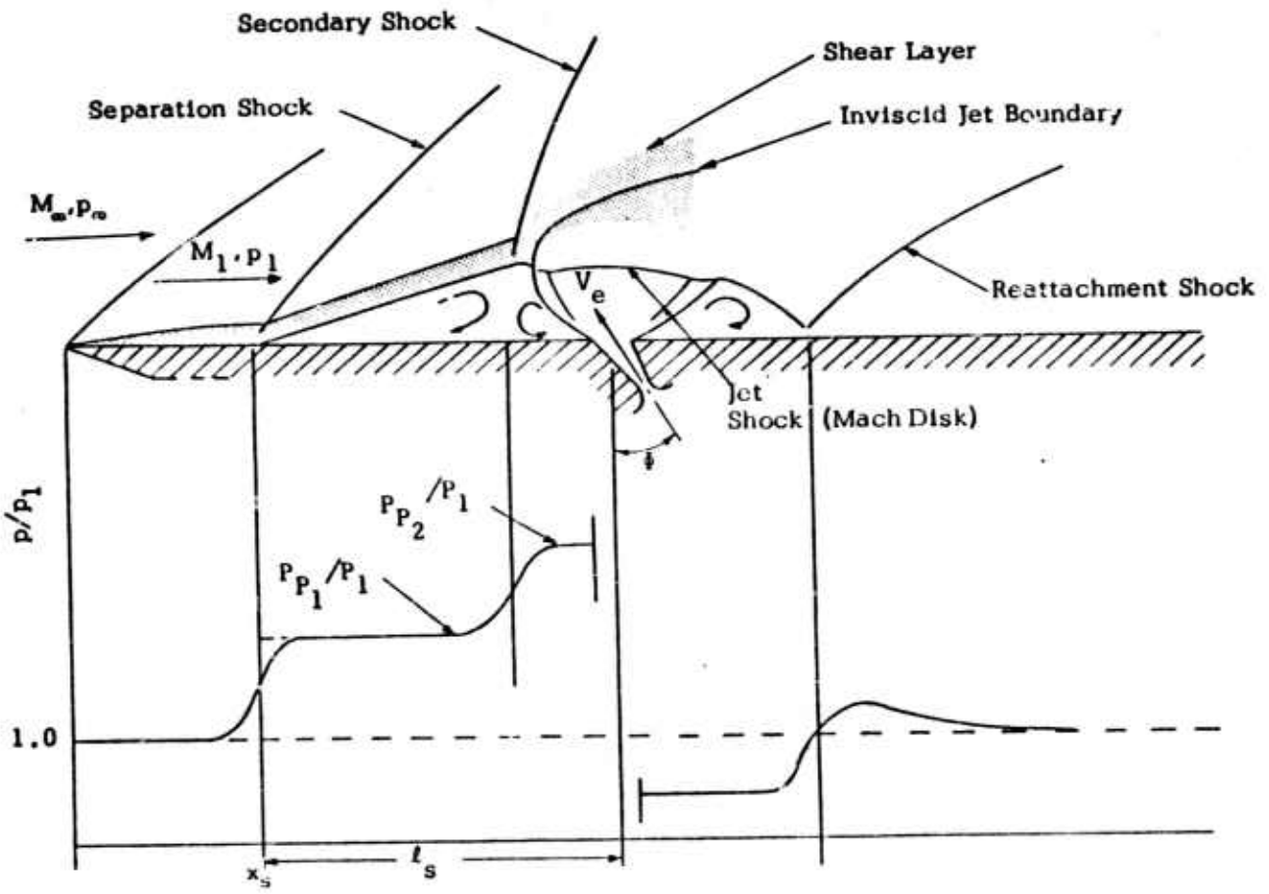

Figure 27. Two-Dimensional Jet Interaction Flow Geometry. From [24].

VII. CONTROL DESIGN CALCULATIONS

A. INTRODUCTION

The design calculations for the hypothesized reaction jet control system in the 5"/54 GLM were divided into several major steps. Utilizing the final iteration of the aerodynamic configurations, the coefficient of lift required for the vehicle to execute a 30-g maneuver was determined. From the aerodynamic results for Configuration III, an angle of attack corresponding to the required lift coefficient was calculated. The next step involved calculating the moments resulting from each of the individual lift coefficients corresponding to the nose, body and tail of the GLM. The center of gravity location needed for the moment calculations was assumed. Accurate location of the center of gravity is left to future studies of the GLM. From the moment calculations, the required reaction jet control force was determined, and a graph depicting the reaction jet force as a function of center of gravity location was constructed. Finally, using the two-dimensional theory discussed in Section VI, the required F_j (jet thrust) was calculated. The calculated jet thrust is the value corresponding to the mass flow bled off the ramjet engine for GLM control. The reaction jet control design is sketched in Figure 31.

B. REQUIRED LIFT COEFFICIENT

One of the design specifications for the GLM was that the missile be capable of a 30-g maneuver to intercept a target. The first step in the calculation of the required reaction jet force needed to maneuver the GLM is to determine the required lift (or normal) force coefficient for the missile. As shown in the Appendix, lift is nearly equal to the normal force N when the angle of attack is small and the lift-to-drag ratio is large. Since the conditions of small α and large L/D apply to the GLM, L and N are used interchangeably in this thesis.

From Figure 28 the lift, L, required by the GLM in a constant acceleration turn is

$$L = nmg$$

The maneuver load factor is n, and m is the missile mass, kg.

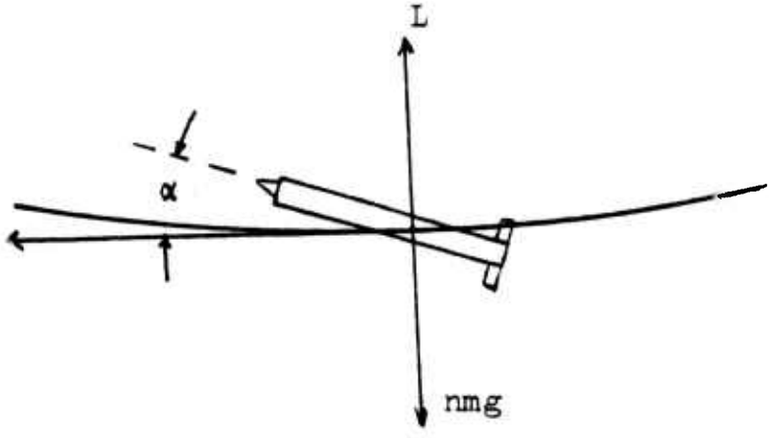

Figure 28. GLM in a constant acceleration turn.

Recall that

$$L = C_L \, qS_r \tag{35}$$

S_r is the reference area for the GLM. The required lift coefficient is

$$C_{Lr} = \frac{nmg}{q \, S_r} \tag{36}$$

Equation (36) gives the lift coefficient needed to develop the required lift for the GLM to maneuver. Since the GLM is considered to be powered to intercept, complete burn of the rocket fuel and 0.85 burn of the ramjet fuel were used in the calculation. For the calculations, values for the mass of rocket fuel and the mass of the ramjet fuel were obtained from Brown's [4] investigation of ramjet propulsion. The weight of the rocket exhaust nozzle was used in the calculation since upon complete burnout of the rocket fuel the nozzle is expended.

Mass (Ramjet fuel) = 3.326 kg

Mass (Rocket fuel) = 5.2512 kg

Mass (Nozzle) = 0.5 kg

Firing mass of the GLM is 47.14 kg. By subtracting the values calculated, the maneuver mass is 38.56 kg.

Design values for maneuver at sea level were inserted into equation (36). C_{Lr} was calculated to be 1.427.

From the lift curve shown in Section V for Configuration III, Figure 19, an angle of attack of 11 degrees is required.

C. CALCULATION OF MOMENTS

The second step in the calculation of the required reaction jet force involved the calculation of the moments coincident to each of the individual lift coefficients corresponding to the nose, body and tail of the GLM.

Figure 29 shows the location of the individual component lift coefficients for Configuration III. Distances in the calculations were measured from the nose tip of the GLM.

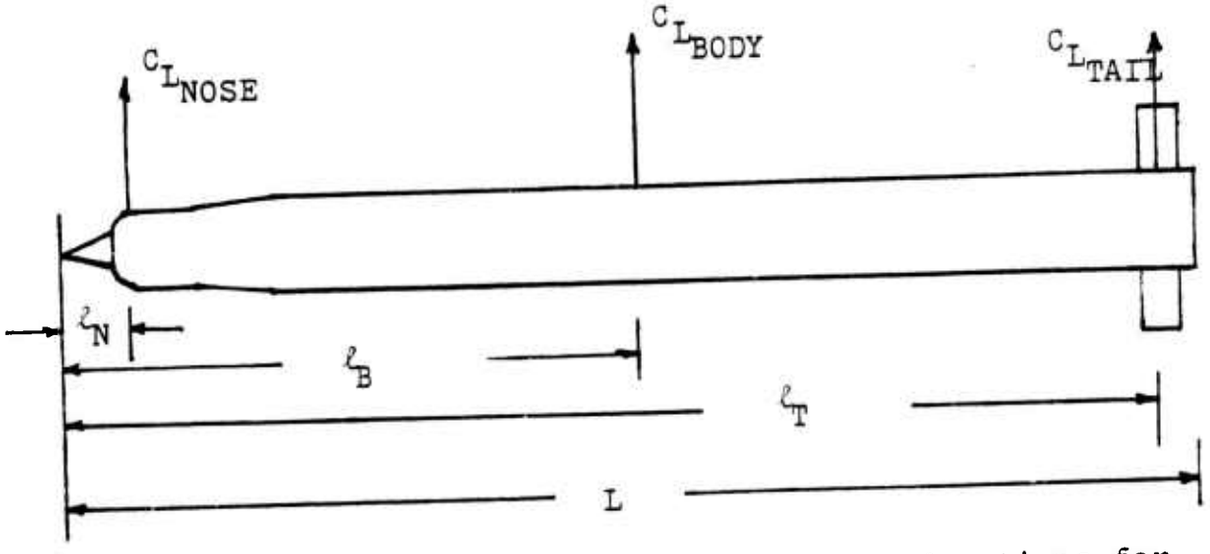

Figure 29. Lift (normal force) coefficient locations for Configuration III.

Because the reaction jet force was to be interdigitated between the tailfins, the distance of this force from the nose tip was equated to that of the component force due to the tailfins. The component of lift due to the configuration "bottleneck" was incorporated into the component of force due to the nose itself, as discussed in the theory

The overall length of the GLM, L, and measured distances as depicted in Figure 29 from the nose are:

$$L = 1.5494 \text{ m.}$$

$$\ell_N = 0.1016 \text{ m.}$$

$$\ell_B = 0.7049 \text{ m.}$$

$$\ell_T = 1.5176 \text{ m.}$$

The center of gravity location x_{cg} was assumed to be one half the length of the GLM for the initial calculation. For more accurate determinations, a plot of the force due to the reaction jet required to trim the GLM for a 30-g maneuver at Mach 3.0 and at sea level was made.

$$x_{cg} = 0.7747 \text{ m.}$$

From the Configuration III aerodynamic data, the component force coefficients for lift were determined to be

$$C_{L_N} = 0.384$$

$$C_{L_B} = 0.978$$

$$C_{L_T} = 0.299$$

for the required angle of attack α for the 30-g maneuver.

For each component force coefficient of lift, the corresponding moment coefficient C_M was

$$C_{Mj} = C_{Lj} \left(x_{cg} - \ell_j \right) \tag{37}$$

where the index j indicates nose, body, tail or reaction jet. Inserting the values for each component of lift into equation (37):

$$C_{M_N} = 0.2585$$

$$C_{M_E} = 0.0683$$

$$C_{M_T} = -0.2221$$

For the GLM to be trimmed at the angle of attack required for the 30-g maneuver

$$C_{M_N} + C_{M_B} + C_{M_T} + C_{M_{rj}} = 0 \qquad (38)$$

where $C_{M_{rj}}$ is the moment coefficient required of the reaction jet side force.

By retracing the calculations for the given location of the reaction jet control orifices, the side force can be found. Using equation (37)

$$C_{L_{rj}} = C_{N_{rj}} = 0.1410$$

and

$$\text{Force}_{rj} = C_{N_{rj}} qS_r = 1122.6 \text{ N}$$

For a given center of gravity and reaction jet moment coefficient required, the reaction jet force has been calculated. The required forces due to the reaction jet have been plotted in Figure 30.

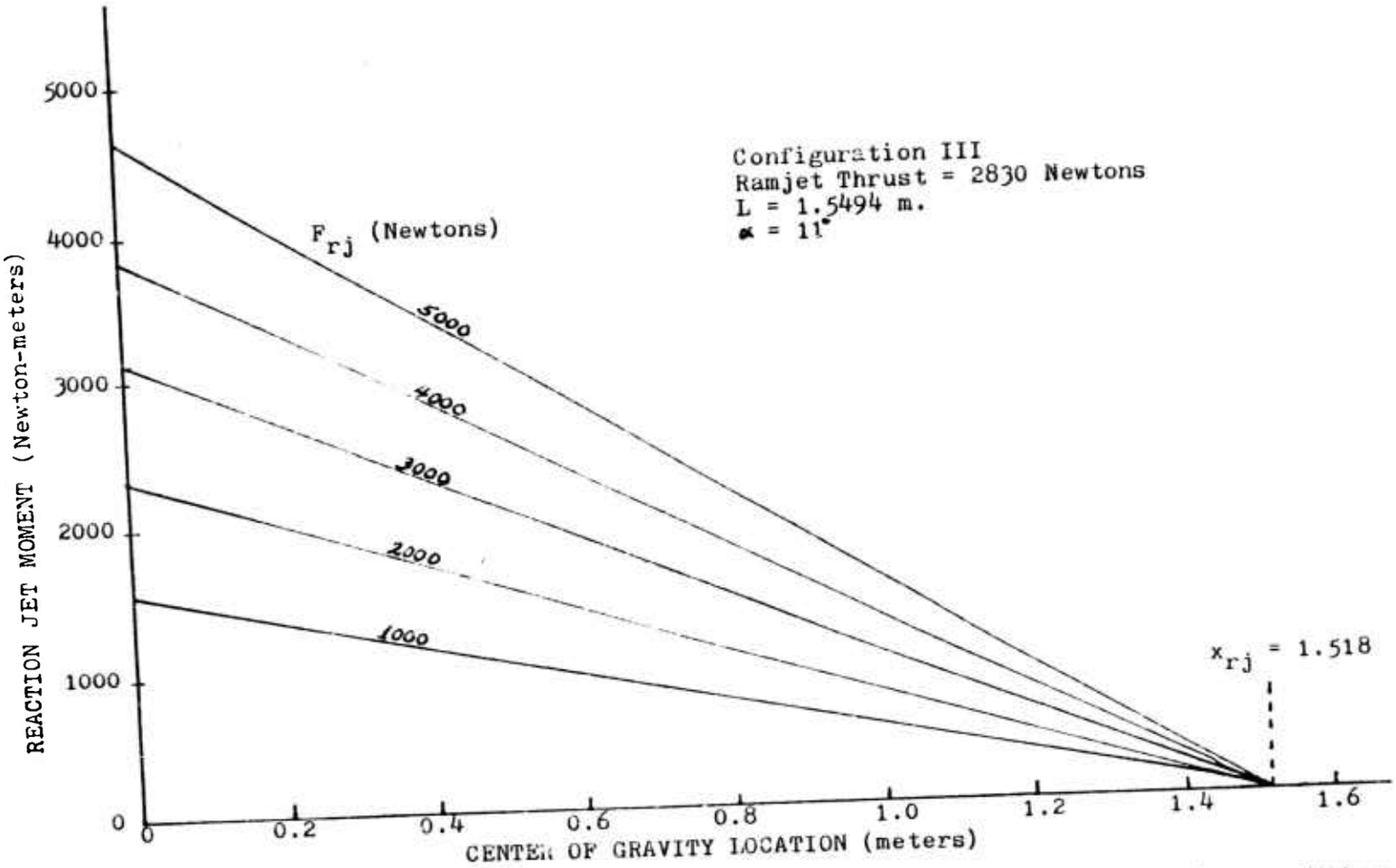

Figure 30. Moment due to reaction jet control as a function of the position of GLM center of gravity with reaction jet control force as a parameter required to trim GLM for a 30-g maneuver at Mach 3 and sea level.

D. CALCULATION OF REACTION JET THRUST

From the theory, recall that the side force normal to the body was not equal to the actual reaction jet force but in fact was greater by an amplification factor K [21, 24]. Based on the tabulated results from the Levine study [24], the amplification factor for the GLM design was conservatively assumed to be two. Nunn [22] states, however, that three as an amplification is not unreasonable for the two-dimensional approximation. The reader is referred to Refs. [21-24] for more information. Thus, for K = 2 the reaction jet thrust needed for the 30-g maneuver is

$$F_j = F_{rj}/K = 561.3 \text{ Newtons}$$

The jet thrust is that force which is result of the mass bled from the ramjet engine. Figure 31 depicts a preliminary design sketch of the reaction jet control orifices interdigitated between the tailfins. Orifices would be located 45 degrees between fins.

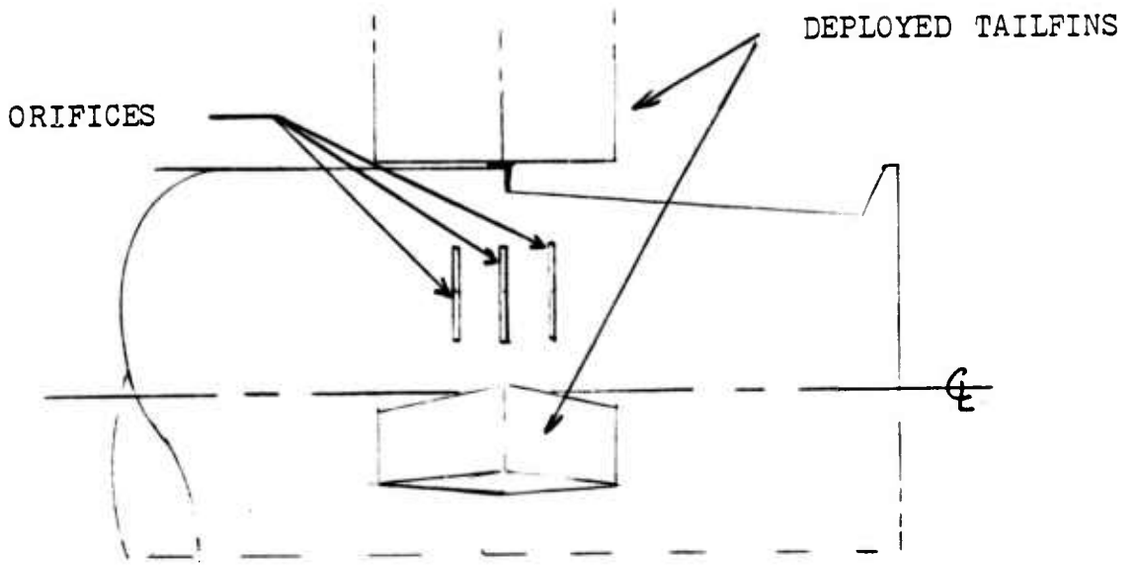

Figure 31. Reaction jet control orifices located between tailfins of Configuration III.

VIII. CONCLUSIONS

A. AERODYNAMIC CONCLUSIONS

The following aerodynamic conclusions were reached as a result of this study:

1. The drag coefficient increased from Configuration I through Configuration II to Configuration III. Lift-to-drag ratio decreased from Configuration I through II to III.
2. Gun-launched missile volume increased from Configuration I to II but decreased slightly in Configuration III.
3. The calculated center of pressure was found to be aft of the estimated center of gravity for a Mach 2.0 launch from the gun. The margin of stability was 3 percent of the length of the GLM.

B. REACTION JET CONTROL CONCLUSIONS

The following reaction jet control conclusions were reached:

1. The total force of reaction control jet thrust required to trim the GLM to 11 degrees angle of attack for a 30-g maneuver at sea level Mach 3.0 is 561.3 Newtons. The amplification was assumed to be 2.
2. The static pressure in the chamber for Mach 3.0 as determined by Brown [4] is 2,137,873 N/m^2.
3. The percentage bleed of the ramjet airflow required for the reaction jet control is 19 percent. Ramjet design did not include this bleed.

APPENDIX

RELATION BETWEEN AERODYNAMIC FORCES

The purpose of this appendix is to clarify the relation between aerodynamic forces on a flight vehicle. Figure 32 helps depict the situation.

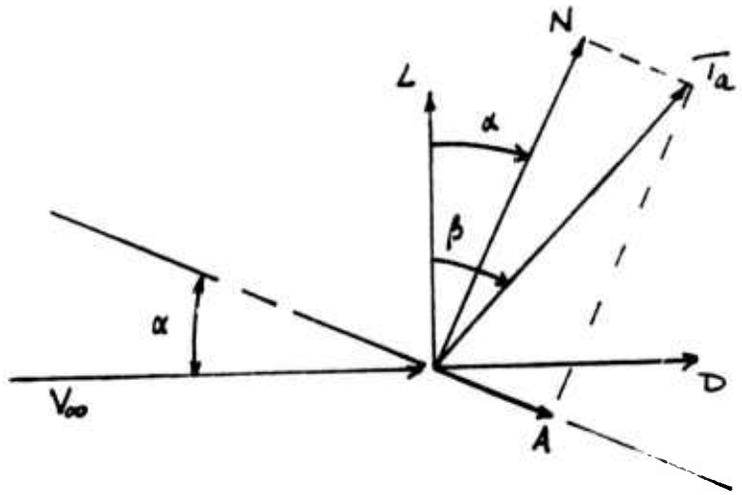

Figure 32. Relation between aerodynamic forces.

In Figure 32, the following symbols are defined:

V_∞ - freestream velocity vector

L - aerodynamic lift which is normal to V_∞

D - aerodynamic drag which is parallel to V_∞

N - aerodynamic normal force which is normal to the missile axis

A - aerodynamic axial force which is parallel to the missile axis

T_a - total aerodynamic force

From the geometry of Figure 32,

$$T_a = L^2 + D^2 = L\sqrt{1 + (D/L)^2} \qquad \text{(A-1)}$$

and likewise

$$\beta = \tan^{-1} D/L \qquad \text{(A-2)}$$

If, from the geometry, the aerodynamic normal force, N, which is normal to the missile axis is equal to the total aerodynamic force T_a multiplied by the cosine of β minus α then, by substituting equation (A-1) and by the use of a trigonometric identity

$$N = L\sqrt{1 + (D/L)^2}\ (\cos\beta\cos\alpha + \sin\beta\sin\alpha) \qquad \text{(A-3)}$$

But from the geometry of Figure 32, equations (A-4) and (A-5) can be seen.

$$\cos\beta = \frac{1}{\sqrt{1 + (D/L)^2}} \qquad \text{(A-4)}$$

$$\sin\beta = \frac{D/L}{\sqrt{1 + (D/L)^2}} \qquad \text{(A-5)}$$

By substitution of equations (A-4) and (A-5) into equation (A-3), equation (A-6) can be found.

$$N = L\sqrt{1 + (D/L)^2}\left[\frac{\cos\alpha}{\sqrt{1 + (D/L)^2}} + \frac{(D/L)\sin\alpha}{\sqrt{1 + (D/L)^2}}\right]$$

and

$$N = L(\cos\alpha + D/L\sin\alpha)$$

Hence for small α and large L/D, N = L. From Figure 32 the axial force A is

$$A = T_a \sin (\beta-\alpha) \qquad \text{(A-8)}$$

Combining equations (A-1), (A-4), (A-5) and (A-8) yields

$$A = L \ (D/L \cos\alpha - \sin\alpha) \qquad \text{(A-9)}$$

For situations of a small angle of attack α and a large L/D, A = D.

LIST OF REFERENCES

1. Jane, F.T., Jane's Fighting Ships, 1980-1981 ed., Jane's Publishing Co., 1980.

2. Parks, W., Warhead Design of a Ramjet Propelled 5"/54 Guided Projective for use in Anti-Ship Missile Defense, M.S. Thesis, Naval Postgraduate School, Monterey, California, December 1980.

3. Frazier, R., Exterior Ballistics, Guidance Laws and Optics for a Ramjet Propelled Gun-Launched Missile, M.S. Thesis, Naval Postgraduate School, Monterey, California, December 1980.

4. Brown, G.L., Propulsion for Ramjet Propelled Guided Projectile for 5"/54, M.S. Thesis, Naval Postgraduate School, Monterey, California, December 1980.

5. Neilsen, Jack N., Missile Aerodynamics, McGraw-Hill, 1960.

6. Hoerner, Sighard F., Fluid-Dynamic Lift, Chps, 3, 19, Hoerner, 1972.

7. Liepmann, H.W. and Roshko, A., Elements of Gasdynamics, pp. 107-108, John Wiley and Sons, Inc., 1957.

8. Tillotson, K. and Schonberger, J., "Supersonic Flow about a Yawed, Slender, Pointed Body of Revolution", computer program developed at Naval Postgraduate School, October 1980.

9. Hoerner, Sighard F., Fluid-Dynamic Drag, Chps 3, 15, Hoerner, 1965.

10. Bertin, J.J. and Smith, M.L., Aerodynamics for Engineers, pp. 22, 323-326, Prentice-Hall, Inc., 1979.

11. Rotty, R.M., Introduction to Gas Dynamics, pp. 147-159, Wiley, 1962.

12. Talay, Theodore A., Introduction to the Aerodynamics of Flight, p. 44, National Aeronautics and Space Administration, SP-367, 1975.

13. Course AE 4705, Naval Postgraduate School, 1979.

14. Rosenhead, L. and others, A Selection of Tables for use in Calculations of Compressible Airflow, Oxford 1952.

15. Garnell, P. and East, D.J., Guided Weapons Control Systems, p. 33, Pergamon Press, 1977.

16. Zukoski, Edward E., and Spaid Frank W., "Secondary Injection of Gases into a Supersonic Flow," AIAA Journal, Vol, 2, No. 10, pp. 1689-1690, October 1964.

17. . . . . ., "A Study of the Interaction of Gaseous Jets from Transverse Slots with Supersonic External Flows", AIAA Journal, Vol. 6, No. 2, pp. 205-212, February 1968.

18. Chambers, R.A. and Collins, D.J., "Stagnation Temperature and Molecular Weight Effects in Jet Interaction", AIAA Journal, Vol. 8, No. 3, pp. 584-586, March 1970.

19. Koch, Larry N., and Collins, D.J., "Variation in Secondary Mach Number and Injection Angle in Jet Interaction," AIAA Journal, Vol. 9, No. 6, pp. 1214-1216, June 1971.

20. Young, Carl T.K., and Barfield, B.F., "Viscous Interaction of Sonic Transverse Jets with Supersonic External Flows," AIAA Journal, Vol. 10, No. 7, p. 583, July 1973.

21. Wu, J.C. and others, "Experimental and Analytical Investigations of Jets Exhausting into a Deflecting Stream," Journal of Aircraft, Vol. 7, No. 1, p. 44, January 1970.

22. Nunn, Robert H., "Jet-Interaction Wrap Around on Bodies of Revolution," Journal of Spacecraft and Rockets, Vol. 7, No. 3, p. 334, March 1970.

23. Grunnet, James L., "Factors Affecting the Magnitude of Jet Interaction Forces," Journal of Spacecraft and Rockets Vol. 8, No. 12, p. 1234, December 1971.

24. Naval Weapons Center Technical Paper 4839, Jet Interaction Performance of Tactical Missile Configurations for Project Quickturn (U), by J.N. Levine, pp. 12-21, April 1970. (CONFIDENTIAL Document).

INITIAL DISTRIBUTION LIST

		No. Copies
1.	Defense Technical Information center Cameron Station Alexandria, Virginia 22314	2
2.	Library, Code 0142 Naval Postgraduate School Monterey, California 93940	2
3.	Department Chairman, Code 67 Department of Aeronautics Naval Postgraduate School Monterey, California 93940	1
4.	Distinguished Professor A.E. Fuhs Code 67Fu Department of Aeronautics Naval Postgraduate School Monterey, California 93940	10
5.	LTC Jean Reed Defense Advanced Research Projects Agency 1400 Wilson Blvd. Arlington, Virginia 22209	2
6.	Commander, Naval Sea Systems Command Naval Sea Systems Command Headquarters Attn: Code 62YC Washington, D.C. 20362	1
7.	Mr. Conrad Brandts Naval Surface Weapons Center Dahlgren, Virginia 22448	1
8.	Dr. Gordon Dugger Applied Physics Laboratory Johns Hopkins Road Laurel, Maryland 20810	1
9.	Dr. Fred Billig Applied Physics Laboratory Johns Hopkins Road Laurel, Maryland 20810	1

10. Department Chairman, Code 69 — 1
Department of Mechanical Engineering
Naval Postgraduate School
Monterey, California 93940

11. Professor G.H. Lindsey, Code 67 — 1
Department of Aeronautics
Naval Postgraduate School
Monterey, California 93940

12. LCDR John S. White, USN — 1
2712 Olive Street
Texarkana, Texas 75501